

# An Overview of Microwave Imaging for Breast Tumor Detection

Ria Benny\*, Thathamkulam A. Anjit, and Palayyan Mythili

**Abstract**—Microwave imaging (MWI) is a non-ionizing, non-invasive and an upcoming affordable medical imaging modality. Over the last few decades, MWI has invited active research towards bio-medical imaging, with special focus on breast tumor detection. After long years of intense research and clinical trials, a breast tumour monitoring unit based on MWI is finally entering clinical imaging scenarios. In this manuscript, the vast literature in MWI to date has been consolidated, and an in-detail study of the state-of-the-art for breast tumor detection has been presented. The hurdles faced during clinical trials are discussed, and their possible solutions and future directions for a fast transition into clinical imaging have been presented. It is hoped that this paper can serve as a guide for MWI researchers and practitioners, especially those new to the field to comprehend the potential of MWI as a viable imaging tool for breast imaging.

## 1. INTRODUCTION

Medical imaging involves the visualization of the human body, which can act as a guide for clinical diagnosis and medical intervention purposes [1]. These imaging techniques aid in obtaining an overview of the internal functioning non-invasively. Medical imaging using microwaves is a promising technology for imaging the human body in a safe, non-ionizing, and low-cost manner.

Microwave imaging is being developed by researchers for breast imaging and other biomedical imaging applications. Breast cancer is the most commonly diagnosed cancer in women and also has the highest chance of incidence [2]. According to the American Cancer Society (ACS), breast cancer makes up 25% of all new cancer diagnoses among women globally. A crucial point noted from the statistics is that the five-year survival rate for breast cancers detected at an early stage is 80–90%, falling to 24% for those diagnosed at an advanced stage [3]. Thus, an early stage detection is vital, which calls for a safe and cost effective imaging technique.

The current assessment protocol for the evaluation and characterization of palpable breast lump primarily involves the triple assessment, which involves a three-step process of physical examination, mammography, and Fine Needle Aspiration Cytology (FNAC). Screening mammography uses ionizing X-rays for imaging, involves painful breast compression, and also has a high false negative rate (4–34%) and high false positive rate (70%) [4]. FNAC is an invasive step and can only provide the cell cytology information and a suggestive nature of the tissues involved. Ultrasound (US) imaging is a safe imaging technique often used as a supplement to mammography. US has been reported to diagnose cancers at an earlier stage than mammography, and it has a higher sensitivity in comparison to mammography in dense breast cases [5]. This improved cancer detection rate of US comes at the cost of an increased false detection rate. This results in unnecessary biopsies and interventions and also has an adverse psychological impact on patients. Additionally, US is highly operator dependent, and it hardly shows any micro-calcification which is an important sign of breast cancer [6]. The other prevalent imaging modality is Magnetic Resonance Imaging (MRI) which cannot be used for regular screening as it is expensive,

---

*Received 24 January 2020, Accepted 14 April 2020, Scheduled 6 May 2020*

\* Corresponding author: Ria Benny (riabenny2802@gmail.com).

The authors are with the Cochin University of Science and Technology, Cochin, Kerala, India.

time consuming (20–90 minutes), and claustrophobic. MRI is also contraindicated in pregnant women and in patients having pacemakers and other implants. PET (Positron Emission Tomography) scan is generally a full-body scanning method applied to breast imaging for the confirmation of a tumor detected by mammogram or for treatment monitoring. However, they may fail to detect small tumors (less than 7 mm) and slow-growing, less active tumors. PET scans can sometimes show areas of high activity like rheumatoid arthritis or tuberculosis which may be mistaken for cancers [7]. PET scans are expensive, and they also involve the injection of radioactive tracers which is contraindicated for pregnant women.

MWI on the other hand uses microwave radiations which are safe for exposure as compared to the ionized X-rays used in mammography, CT-scans, etc. MWI sends out very low levels of microwave energy [8, 9] which is below the whole body averaged SAR (Specific Absorption Rate) limit of 0.08 W/kg set by the IEEE/ANSI/FCC and ICNIRP standards [10, 11]. Additionally, MWI avoids the painful breast compression involved in mammography. MWI also avoids the injection of contrast agents like gadolinium used in MRI scans that is contraindicated for kidney patients, pregnant women, etc.

Many researchers have contributed towards the development of this modality. The ability of microwaves to penetrate and image biological objects was demonstrated by Larsen and Jacobi through the imaging of canine kidneys [12]. From the promising results obtained, a major interest was initiated in using microwaves for imaging applications. The efforts towards MWI branched out into two directions:- quantitative imaging and qualitative imaging under the tomographic, radar, and holographic domains. Tomographic methods generate a contrast profile which may be used to estimate the dielectric properties (permittivity/conductivity) of the object under test, resulting in quantitative reconstruction. On the other hand, radar methods produce qualitative reconstruction, which can only identify and locate strong scatterers inside the object under study as can be seen from Figure 1 [13, 14]. Holographic imaging involves the recording of the interference pattern or the ‘hologram’ and the reconstruction of this hologram using a reference signal. Holographic imaging based on quantitative and qualitative reconstruction methods has been developed over time (discussed in Section 3.3).

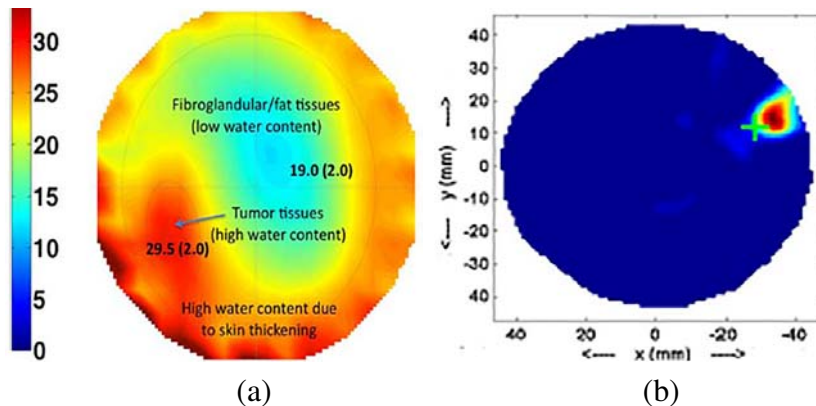


**Figure 1.** Typical outputs produced by (a) quantitative imaging showing the complete dielectric profile obtained [13] and by (b) qualitative imaging showing the tumor detection and localization alone [14].

Although MWI started off as an imaging tool for breast tumor detection, brain imaging for tumor/stroke/hemorrhage detection is a key area of research these days [15, 16]. Their applications of MWI are being explored which include detection of pulmonary edema [17], skin cancer [18], intracranial hemorrhage [19], heel bone fracture [20], cervical myelopathy [21], leukemia [22], cerebral edema [23], lung cancer [24], heart imaging [25], joint tissue imaging [26], thermo-acoustic imaging of subcutaneous vasculature [27], etc.

Many prominent researchers in the MWI field had reported with regret that even after 30 years of intense research, MWI remained to be only a promising imaging modality in a clinical-acceptance phase [28–30]. However, the scenario is rapidly changing, and the long-awaited entry of MWI into practical imaging of hospital patients was initiated in June 2019 with the MARIA imaging system

developed by Micrima Ltd. being installed in hospitals in Germany for breast tumor detection [31].

In this paper, an effort has been made to consolidate the vast literature pertaining to the development of MWI. The key aspects of MWI have been thoroughly studied. The pros and cons of various approaches have been detailed, and the feasible future prospects are discussed. The state-of-the-art clinical studies in breast imaging (11 research teams) have been analyzed in detail. Such a detailed review of MWI is specially relevant in the current scenario with the entry of MWI into actual clinical practice. Section 2 discusses the contributions made by researchers in identifying the basis of MWI technique, i.e., the contrast in dielectric properties of normal and abnormal tissues. In Section 3, the various directions along which research in this field progressed have been examined. Section 4 gives an elaborate description about the imaging systems undergoing clinical trials and their transition into practical imaging for breast tumor detection applications. The hassles that were faced while performing practical trials and the possible approaches to overcome these issues in future are suggested in Sections 5 and 6. Finally, Section 7 concludes this paper.

## 2. DIELECTRIC PROPERTY CONTRAST: THE BACKBONE OF MWI

The driving force behind the competence of MWI in tumor detection is the large difference in the electrical properties (relative permittivity and conductivity) between the malignant and normal tissues at microwave frequencies [32]. The reason behind this contrast in dielectric constant values between different tissue types is the water content present in them. High-water-content tissues (malignant tumors) have higher relative dielectric permittivity and conductivity whereas low-water content tissues (fat) which is abundant in normal breast tissue have lower permittivity [33].

Many studies have been undertaken to achieve dielectric quantification as it helps in the development of accurate numerical models and phantoms for experimental imaging studies [34]. Such dielectric studies were performed in two ways: *ex vivo* methods, which used tissues excised during cancer removal or tissue reduction surgeries [33], and *in vivo* methods, which involved indirect estimation of tissue parameters from a tomography-generated profile or by using probes inserted into the body [35].

*Ex vivo* studies were taken up by various research teams from the 1980's. Chaudhary et al. and Joines et al. reported high permittivity contrast of 3–5 times and 2–5 times respectively between malignant and normal tissues [36,37]. Campbell and Land and Hurt et al. took various large scale *ex vivo* studies [38,39] with an aim to verify the presence of large permittivity differences. However, their findings contradicted the claims of very high dielectric contrast made by early researchers. A minimum contrast of 1 : 1.1 for tissues with less than 30% adipose content was reported by [40,41] as against the worst case levels of 1 : 2.3 envisaged by historical works. The reason for this variation was attributed to the heterogeneous nature of the breast and the presence of fibro-glandular tissues. Though majority of the breast volume is composed of adipose tissues having high dielectric contrasts as compared to malignant cells, tumors usually sprout out from regions in and around the fibro-glandular connective tissues possessing only around 10% variation in permittivity [42]. The relief for researchers was that this low contrast was just the worst case scenario in MWI, whereas the breast imaging standard, mammography handled contrasts as low as 4%.

In the meantime, *in vivo* studies were taken up, and they showed that the breast had a very heterogeneous structure. It was reported that the contrast between normal fibroglandular tissues and malignant tissues was smaller than the contrast of malignant cells from adipose tissues, but greater than that reported by Lazebnik et al. [41]. This has helped to overcome the confusion about the viability of MWI for tumor detection. Moreover, the Micrima group was able to implement the automatic discrimination of *in vivo* assessed lesions from a limited number of parameters extracted from the dielectric radio-frequency response [35]. Chung et al. further experimentally found that malignant tissues had higher fraction of free water than normal tissues and introduced Bound Water Index (BWI) as a noninvasive *in vivo* index for tissue distinction [44].

Various researchers experimentally determined the reason for the small contrasts reported in ex-vivo studies by [38–41]. In 2016, Farugia et al. concluded from experiments on lung tissue that dehydration of the excised tissues is the major contributor to the low contrasts [32]. In 2017, Shahzad et al. also reported that a change of more than 25% in both the real and imaginary parts of complex permittivity occurs in tissues over 3.5 hours after excision [45]. Another source of error in *ex vivo* experiments was

seen to be the use of an open-ended coaxial probe for measurements. The long-held presumption among researchers was that an open-ended dielectric probe provides an accurate estimate of tissue properties over a heterogeneous sensing volume 2 mm to 3 mm below the surface of the probe. However, Meaney et al. studied the sensing volume of such probes [46] and found that the material within the first few hundred microns exerts the dominant influence [46]. Thus, for reliable results, the tissue content may need to be weighted by distance from the probe. In 2018, the team developed a transmission-based dielectric probe with a sensing depth as large as 1.5 to 2 cm compared to 0.3 mm for conventional probes [47]. The developed probe was also less affected by measurement technique variability. Further, Porter et al. [49] observed that histology depth (defined as the depth to which the probe can detect changes in the tissue sample within the measurement uncertainty) varies with frequency, and hence, it should have been included as a con-founder in historic data sets (like Lazebnik et al.) where the histology depth was taken as a constant value. In 2018, it was further noted that the probe sensing radius could be smaller than the probe radius and depended on the histology of the tissue sample [48]. MINDER (Minimum Information for Dielectric Measurements of Biological Tissues) model was developed by the team which allows to reproduce measurements, provides ease of interpreting and reusing data, and comparison of data across studies [49].

In-vitro spectroscopy was also adopted by researchers to quantify the actual tissue dielectric values. In 2017, experiments performed by Zubair et al. showed that the contrast between normal and malignant tissues was sufficient to enable tumor detection [50]. Again in 2019, Hussein et al. performed microwave spectroscopy of normal and breast cancer cell lines cultured in vitro. The main advantage of using cell lines is that when being grown in a standard medium, they provide an unlimited supply of self-replicating homogeneous cell population [51]. The analyzed breast cancer cell lines exhibited higher dielectric properties than healthy cells. This significant dielectric contrast between normal and cancer cells underlines the ability of MWI to carry out reliable breast tumor detection.

Hence, on the whole it can be suggested that, in future, dielectric studies must be taken in accordance with the latest principles by accounting for all confounders to understand the dielectric contrast in exact figures. Reported results that tissue dehydration reduces dielectric values by about 25% within 3.5 hours after excision [45], that sensing depth varies with frequency and hence is not to be taken as a constant [48], that permittivity drops 0.13% per degree Celsius [52], that sensing radius is not restricted to be larger than probe radius [48], etc. must all be taken into consideration during data collection and interpretation to arrive at the final result.

### 3. CLASSIFICATION OF MWI TECHNIQUES

The existence of contrast in dielectric properties between the healthy and malignant tissues led early researchers to build passive imaging systems that were later replaced by active imaging setups. Active imaging methods can be classified into tomography, radar, holographic and hybrid imaging techniques as depicted in Fig. 2.

**Tomography:** Tomographic imaging provides a quantitative description of the permittivity and conductivity distribution of the organ under evaluation. It is carried out in two levels. The first step involves the illumination of the object under study from probing antennas placed around the object and gathering the scattered signals, termed as data acquisition phase or measurement phase (forward problem). Next step involves solving the complex inverse problem to yield the dielectric distribution.

**Radar-based imaging:** Microwave radar imaging was first developed as a military ground-penetrating application, and later applied to the human body. This methodology reconstructs the image from the waves reflected off the surface of the organ under study. It obtains a qualitative reconstruction of the tissues by detecting and locating the tumor bodies inside.

**Holographic imaging:** This method is based on the hologram technique in optics. Here, the hologram of the object is illuminated with a reference signal to generate a three-dimensional (3D) view. Holographic imaging can be carried out using direct or indirect techniques, while direct holography uses two different signals, one for illumination and the other as a reference wave, and indirect holography derives the reference signal from the illuminating source itself.

**Hybrid Imaging:** To compensate the shortcomings of conventional imaging modalities like MRI, mammography, etc. efforts were taken to incorporate MWI techniques into them. Such hybrid systems

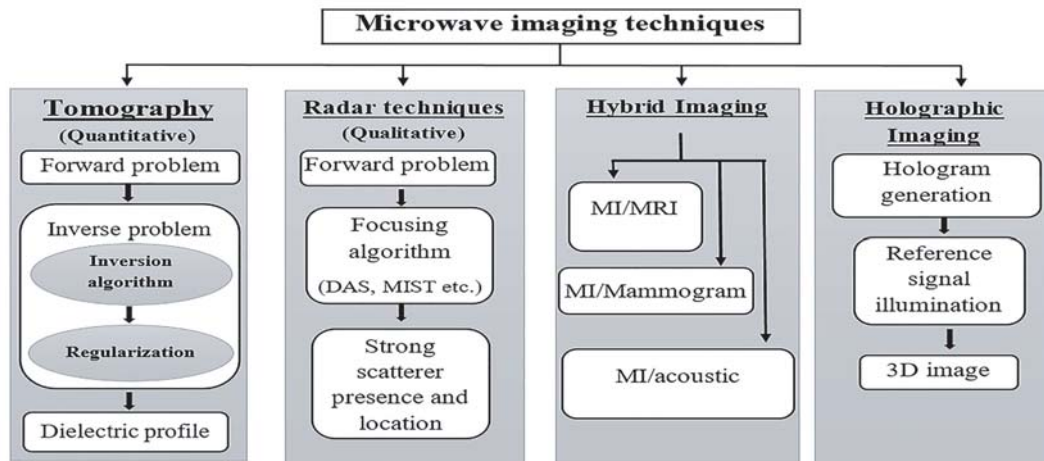


**Figure 2.** Flow diagram depicting classes of MWI: tomography, radar, hybrid & holographic methods.

can help to improve the reconstruction quality.

Tomographic, radar, holographic and hybrid techniques are investigated, and the relevant details are presented in Sections 3.1, 3.2, 3.3, and 3.4. The features of the prototypes developed, the reconstruction algorithms available, the limitations and future options are all thoroughly evaluated.

### 3.1. Tomographic Imaging

The basic advantage of tomographic systems is that the complete information about the dielectric properties of the tissue being imaged is made available upon reconstruction. However, the main hurdle lies in finding the solution to the complex inverse problem. Fig. 3(a) depicts the steps involved in tomographic imaging.

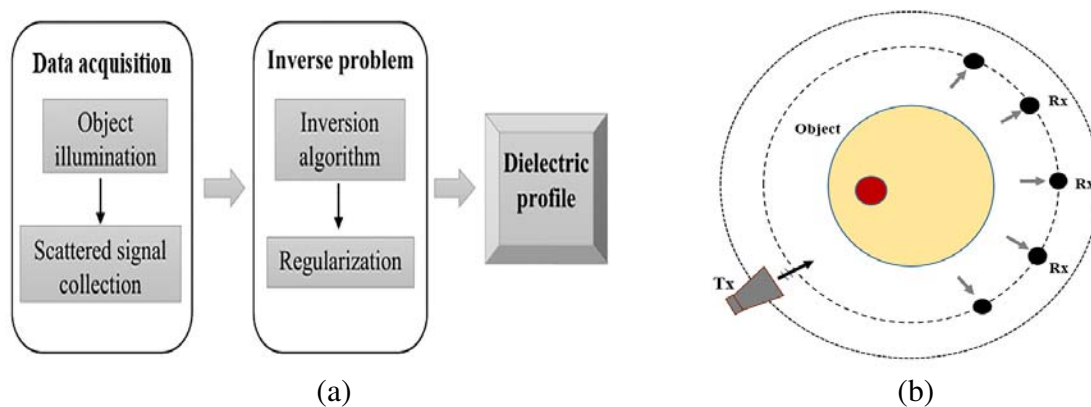


**Figure 3.** (a) Various stages in tomography and (b) circular arrangement of antennas.

#### 3.1.1. Imaging Systems

The tomographic methods initially employed diffraction tomography with the probing antennas placed on a straight line on one side of the object and scattered radiation collected on the other side. Later, it was found that diffraction tomography was effective only for those imaging scenario which involved weak scatterers (with a small variation in dielectric contrast values). Moreover, the placement of antennas on a straight line yields meagre amount of information for reconstruction [53]. Hence, tomography-based systems started using a circular arrangement (Fig. 3(b)).

Semenov et al. developed the initial experimental setups in a circular configuration capable of performing complete 3D acquisition [54]. The next major step was the development of a 64-antenna 2.33 GHz camera by Joise et al. in 1999 which generated a 2-D cross-section of the arm [55].

The first clinical prototype for tomographic imaging of the breast was developed by Dartmouth group in 2000 [56] which operated in the 300 MHz to 1 GHz frequency range. The refined imaging unit is presently engaged in clinical trials. Another imaging unit presently engaged in clinical trials was made in 2010 by researchers from the Electronics and Telecommunications Research Institute (ETRI) of Korea [57] which handled the 500 MHz to 3 GHz spectrum. A 3D imaging system designed to work at 3 GHz was developed by Zhurbenko et al. in 2010 with the antennas arranged in the form of a cup into which the patient's breast was to be placed. The setup could complete the acquisition in merely 50 seconds [58]. The drawback was the single frequency approach; it needed to be extended into a multiple frequency approach. Additionally, since the cup housing the antenna-array was of a fixed size, the imaging of patients with varying breast sizes created a problem, i.e., larger breast sizes needed compression while smaller breast sizes introduced gaps and increased losses. Fabrication of a size-adjustable cup could help obtain enhanced measurements.

In 2017, Gibbins et al. built a compact and portable sophisticated structure constituted by an array of Large Cavity-Backed Wide-Slot (LCBWS) antennas working in the 1–4 GHz range [59]. Phantom-based imaging showed good reconstruction quality. The imaging unit is fine-tuned for continuous monitoring of forearm bone health. In 2018, Fedeli et al. reported a prototype with an ad-hoc 3D-printed structure which supports sixteen custom antenna elements. The collected scattered data was inverted by a hybrid algorithm combining qualitative and quantitative reconstruction techniques [60]. Incorporating boundary information of the imaged object as a-priori information helps in better accuracy of recovered images. Hence, a torso-scanner was developed by Zamani et al. in 2018 and improvised in 2019 to carry out 3D electromagnetic scanning for detection of pathologies in the chest and upper abdomen [61, 62]. Again in 2019, the quantitative imaging system developed by Asefi et al. has avoided the use of immersion liquids. Air-based quasi-resonant breast MWI has been attempted successfully by the research team [63].

Researchers have perfected their imaging units to start clinical trials. Many of the systems described above are now undergoing active clinical trials (discussed in detail in Section 4), while others will soon start the trials after successful validation in the ongoing tests with phantoms.

### 3.1.2. Inversion Algorithms

The scattered field data have to be processed using a suitable inversion method to obtain the dielectric profile. These algorithms were introduced by Joachimowicz et al. [64] and Chew and Wang [65] in the beginning of the 1990's. These methods belong to one of the four distinct classes: exact methods, direct approximate methods, direct iterative methods, or optimization methods.

Exact methods have an explicit expression for the unknown and reconstruct the unknown in a finite number of iterations as applicable to one-dimensional cases [66]. Direct approximation methods involve the linearization of the nonlinear inverse scattering problem by the application of Born or Rytov approximations [67]. These schemes are simple to implement but are able to produce only qualitative reconstruction. Direct iterative methods like Born Iterative Method (BIM) [68] and Distorted-wave Born Iterative Method (DBIM) [69] proceed by iterating between the forward and inverse scattering problems until convergence. Upon implementing BIM, it was noted that it may not be the best method to solve the nonlinear inverse-scattering problem because second-order convergence is not offered. Moreover, BIM failed miserably in the presence of strong scatterers with large contrast differences. With DBIM, the background medium is not constrained to be homogeneous. Upon implementing DBIM, it was observed that convergence is attained in much fewer iterations. Moreover, the efficiency in handling strong scatterers was noteworthy.

In the recent literature, it was noticed that improved versions of DBIM with increased convergence rates have been conceived and applied. Subspace DBIM (S-DBIM) and its improved version SDBIM-v2 linearly retrieve the deterministic subspace of the induced current and estimate the total electric field more accurately than DBIM [70]. Yet another upgrade to DBIM was the DBIM-with-Spatial Priors (DBIM-SP) which utilized prior information about the structure of the breast derived from another imaging modality like MRI. Extremely sparse matrices with elements either (+1) or (−1) were made

available for the inversion procedure [71]. Again in 2017, Palmeri et al. developed a virtual-experiment-based DBIM scheme wherein at each iteration, and after the scenario update, the virtual experiment parameters were also redesigned making it more robust than plain DBIM [72].

Optimization methods proceed by constructing a nonlinear cost function from the measured scattered field and the unknown medium properties and minimizing the cost function through methods like conjugate gradient method or its modified versions, Newton-Raphson method or Gauss-Newton method, Inexact Newton methods, etc. Most of the prominent works in MWI especially those employed in clinical trials are based on the Gauss-Newton scheme. To overcome the smoothing effect produced by the basic Gauss-Newton method, Meaney et al. in 2017 introduced a weighted Euclidean distance penalty term to produce quality results [73]. Tournier et al. applied the Gauss-Newton method in synthesizing a Fast-Forward electromagnetic Solver (FFS) [74] and Bisio et al. in 2018 applied the technique towards discriminating the stroke affected areas from the healthy regions [75].

**Remarks:** Based on a thorough investigation, it is observed that either Gauss-Newton method, or DBIM or its improved versions are the best options for inverse profiling. The rate of convergence, computational efficiency, and quality of reconstruction produced by them stand out in comparison to all others.

However, solution-finding using these inversion algorithms is affected by instability issues due to the sparse nature of the inverse problem. Thus, ill-posedness (produced when the number of unknowns is far greater than the number of known parameters) has to be removed by pairing these inversion algorithms with a suitable regularization scheme.

### 3.1.3. Regularization and Optimization Schemes

The regularization techniques help to replace the original ill-posed problem by a well-posed one by incorporating some additional information (a-priori information). The optimization techniques find values of the variables that minimize or maximize the regularized objective function while satisfying the constraints. Optimization schemes can be broadly classified as deterministic and stochastic. In the deterministic approach, the unknowns can be modeled as a deterministic function; whereas in the stochastic approach, random variables are generated, and a probabilistic modeling is adopted [76].

Evolutionary stochastic algorithms have been successfully applied to solve inverse scattering problems due to their hill-climbing capabilities and their ability to arrive at the global optimum. The important techniques under this category include Genetic Algorithm (GA), Particle Swarm Optimization (PSO), differential annealing, Ant Colony Optimizer (ACO), etc. Genetic algorithm was the first population-based stochastic algorithm which was based on the principles of natural selection and genetic pressure [77]. Thereafter, algorithms based on cooperation framework modeling the interaction in a swarm of bees came up with the PSO, ACO, etc. [78]. Donelli et al. employed an artificial bee colony optimizer algorithm to successfully detect tumors embedded in an MRI-derived breast model [79]. In a recent work Salucci et al. have combined PSO technique with a multiresolution technique and have made possible the simultaneous exploitation of multiple samples of the data [80]. However, increased computational complexity is a major disadvantage posed by these methods.

Bayesian methods which are also probabilistic in nature involve small number of control parameters and provide accurate reconstruction. Moreover, as they are computationally efficient and avoid the problem of local minima, they have been experimented with in many recent works [81, 82]. A quest for perfecting better algorithms in the less explored Bayesian domain is a route open to future researchers.

As far as the deterministic approach is concerned, the objective function is usually subjected to some form of minimization. The basic schemes employing the  $l_2$ -norm minimization include Singular Value Decomposition (SVD), Conjugate Gradient Least Squares (CGLS), Tikhonov method [83], etc. The problem with the use of  $l_2$ -norm is that it produces extra smoothness and becomes drastically inefficient when being applied to domains with sharp variations, discontinuities, or sparse content. So, the sharpness provided by  $l_1$ -norm was adopted [84].  $l_1$ -norm-based implementation received a huge support with the advent of Compressive Sensing (CS).

CS is a novel signal processing paradigm which aids recovery of sparse signals of interest from a small set of linear measurements, even when the number of measurements is less than the number of unknowns. Sparsity-promoting regularized approaches have been developed within CS which express the unknown functions as a sparse set of coefficients with respect to an appropriate basis. In fact, the

techniques based upon minimizing the  $l_1$ -norm are the most commonly used CS methods. In order for a system to undergo CS, several conditions must be satisfied. First, the unknown object of interest must have a sparse representation in some known domain [85]. Second, the measurement matrix must fulfill the Restricted Isometry Property (RIP), and third, the imaging system must utilize a reconstruction algorithm that employs a-priori information. However, standard CS techniques cannot be applied to the inverse problem directly. This is because the unknowns (like the target dielectric contrast) are usually not intrinsically sparse. Hence, sparsifying strategies are to be applied to comply with the fundamental CS sparsity assumption. The measurement matrix in the MWI scenario is the Green's matrix which has a definite form, and it is not easy to impose a-priori information upon it. Thus, development of CS-based strategies specifically altered for MWI inverse problems is necessitated.

Various algorithms have been proposed in the CS framework. Candes and Romberg came up with the " $l_1$ -magic" solver. The handled problems belonged to two classes: those recast as linear programs (LPs) and those as second-order cone programs (SOCPs) [86]. Iterative Shrinkage Thresholding Algorithms (ISTA) are gradient-based, where each iteration involves matrix-vector multiplication followed by a shrinkage/soft-threshold step. However, it has been recognized as a slow method [109]. Recently, several accelerated versions of ISTA like Two-step IST (TWIST), NESTA (Nesterov's ISTA), Fast ISTA (FISTA), etc. have been reported [87]. The DBIM-ISTA scheme was modified by Ambrosiano et al. to include an automatic and adaptive selection of multithreshold values which outperformed the standard thresholding implementation [88, 89]. A DBIM-TWIST combination was applied by researchers from King's College, London to develop and validate a 3D experimental setup [90, 91]. An adaptive thresholding method was developed by Zhou and Narayan in 2019, namely, Iterative Method with Adaptive Thresholding for Compressed Sensing (IMATCS) in conjugation with non-decimated wavelet transform [92]. Total variation (TV) CS method developed by Rudin and Osher [93] needs a mention in this context. This CS technique minimizes the integral of the gradient of the contrast function. Innovative variations of the basic TV-CS were proposed with better performances [1] to overcome its slow convergence rates, mainly when a large number of degrees-of-freedom are handled.

In an MWI scenario, acquiring a-priori knowledge about the target is not always possible. Hence, more attention is needed to come up with strategies which can work without any such before-hand information. Color CS proposed by Anselmi et al. was one such attempt where the optimal expansion basis for each imaging case could be obtained without any previous information [94]. Customization of Color CS to realistic scenarios and geometries is currently under development.

Two-dimensional methods are increasingly extended and replaced by 3D modeling techniques. Here the vectorial nature of the fields has to be tackled. 3D forward models and inversion methods implemented within the contrast source inversion framework have been reported in 2019 like Multi-Task Bayesian Compressive Sensing (MT-BCS) [95], Twofold Subspace-based Optimization Method (TSOM) [96], 3D Electrical-Property Tomography (3D-EPT) [97], Newton-CG Method in  $l^p$  Spaces [98], etc. Development of direct 3D models helps in more accurate modeling and imaging. In 3D modeling, significant approximations are usually implemented within the integral equations to reduce the computational burden associated with the Green's function. To avoid the undesirable effects produced by these approximations, Ansari et al. introduced a partial differential equation framework to implement faster reconstructions that is crucial in emergency scenarios like stroke detection [99].

In the meantime, researchers were involved in many diverse activities to simplify the handling of complicated inverse problems. Expansion-based representations employing wavelet [100], cosine spline and truncated cosine Fourier [101], and Fourier Jacobi [102] expansions were used to reduce the number of unknowns being handled. The authors of this paper utilized a mode-matching Bessel function method to identify scatterers with much simpler matrix inversions [103].

It is generally observed that tomographic techniques have a tendency to reconstruct the real part of the permittivity with much greater accuracy as compared to the imaginary part. Islam et al. proposed a solution to mitigate this imbalance by expressing the complex permittivity as a weighted sum of a few pre-selected permittivities (fraction parameters) close to the range of the expected values [104]. The weights were determined after applying Gauss-Newton optimization. Additionally, it is noted that Bevacqua et al. have reported an efficient technique for 3D reconstruction from only amplitude electromagnetic data [105]. Another activity domain aimed at increasing the amount of data at hand for

improving the reconstruction quality employed Transverse Electric (TE) mode illumination alone [106] or along with TM mode illumination [107].

**Open issues in CS:** In spite of the many advantages offered by CS, certain gap areas which need attention are still present in its implementation. Standard CS theory does not always properly exploit all of the a-priori knowledge that is available in imaging applications. Moreover, enforcing RIP condition upon scattered data is not a feasible option. Therefore, systems that can generate sparse data should be developed. Since different scenarios make available different kinds of a-priori data, generalized schemes that can handle any kind of prior information are needed. It may be noted that as Bayesian CS (BCS) methods avoid the need to check the RIP of the kernel operator, they may be adopted to solve this concern [108].

### 3.2. Radar-Based Imaging

Radar imaging provides information about the presence/absence of a tumor and its location. The microwave signals reflected from the object's surface are first collected. The focusing algorithms process these accumulated signals to detect the lesions within.

#### 3.2.1. Signal Acquisition

Radar-based MWI can be done in the frequency domain or time domain. During the early years of research, radar imaging was done by the frequency approach. Many of the systems built using this approach have now matured towards clinical trials. The time domain-based systems on the other hand started coming up in the recent years. They are more cost effective and offer notably reduced scan time.

**Frequency-domain acquisition:** The frequency-domain signal acquisition procedure involves the collection of  $S$ -parameter measurements by devices like the VNA. The signals which are reflected from the breast surface are collected by sweeping frequencies.

The team from Bristol University performed pioneering work in this domain. The first prototype was built in 2009 named MARIA (Multistatic Array Processing for Radiowave Image Acquisition) composed of 31 UWB slot antennas. The array was thereafter expanded to hold 60 antennas elements ( $MARIA^5$ ) and used with an eight-port VNA and 60-way switch matrix to obtain a reduced scan time of just 10 seconds (discussed in Section 4) [109]. Another major contribution came from the University of Calgary team with the development of the Tissue Sensing Adaptive Radar (TSAR) [110]. This TSAR system is currently being perfected by the team through various clinical trials for actual clinical practice.

In 2019, Islam et al. developed a portable breast imaging unit comprising nine side-slotted tapered slot antennas as seen in Fig. 4(a) [111]. The Iteratively Corrected Delay Multiply and Sum (IC-DAS) algorithm played a decisive role in the reconstruction [112]. In 2019, Alqadami et al. reported a wearable imaging system employing flexible wideband antenna array with a metamaterial unit cells reflector [113].

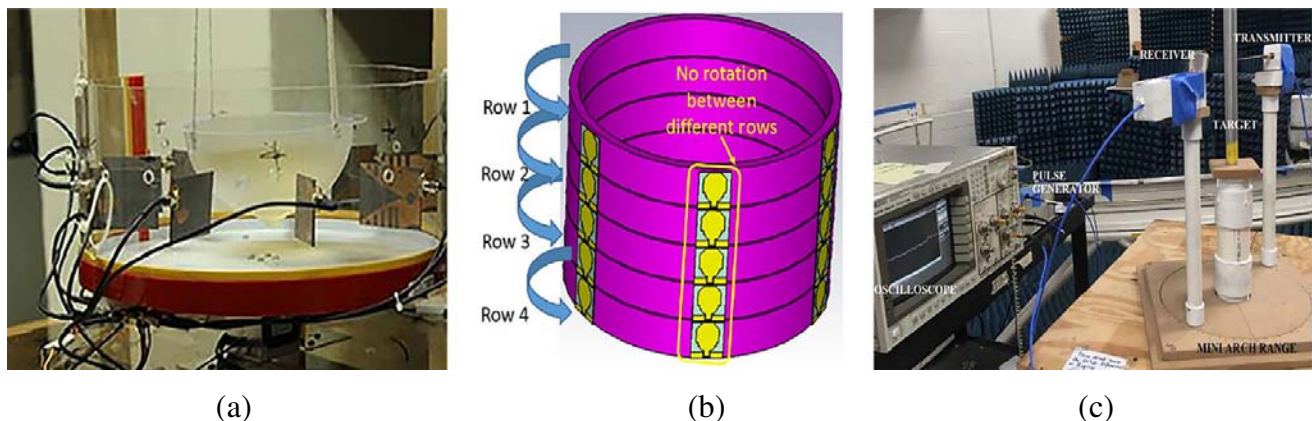


**Figure 4.** Set up used by (a) Islam et al. [111], (b) Wang and Arslan [120] and (b) Mukherjee et al. [122].

Eight such antenna array elements were arranged to image a head phantom that imitates the average real human head properties. Again in 2019, Manoufali et al. proposed three implantable antennas [114] which were used to image the cerebrospinal fluid of piglets, and the antennas were able to sense the variations of the dielectric properties correctly. Felicio et al. assembled a dry contactless imaging setup without the use of any immersion liquid [115]. The radar-based setup based on wave-migration algorithm added to patient comfort and avoided sanitation procedures after each imaging session.

However, the frequency domain techniques need costly and bulky equipment such as a Vector Network Analyzer (VNA). The team from Queensland University, Australia proposed a low-cost reconfigurable microwave transceiver using Software-Defined Radio (SDR) technology as a substitute for VNA [116]. In 2019, the team developed a novel combination of the SDR with a solid-state switching network and a static antenna array to develop a portable multistatic microwave head imaging system [117]. Casu et al. fabricated an FPGA (Field Programmable Gate Array) based circuitry [118] that executed the imaging algorithm 20 times faster than a multicore CPU.

Time-domain acquisition: Time domain systems transmit the input pulse using a pulse generator and receive the signals using an oscilloscope in real time. Additionally, a very fast sampling clock is needed whose design is crucial since even a very small jitter might blur the resultant images. Several research groups have reported time-domain-based MWI systems in the past few years.

The team from McGill University is a leading research group in time-domain measurements [119]. Their experimental setup developed in 2013 was a multistatic radar-based system with a 16-element antenna array which has been refined to enter clinical trials. Wearable bra-type scanning unit was yet another contribution made by them which contained a multi-static time-domain pulsed radar with 16 flexible antennas embedded into a bra. Unlike the previously reported table-based prototype with a rigid cup-like holder, the wearable one required no immersion medium, was significantly more cost-effective, and enabled simple localization of the breast surface. One more wearable type tumor detection assembly proposed by Wang and Arslan from China in 2017 housed 24 UWB flexible antennas arranged in a circular array in four rows [120] as shown in Fig. 4(b). The team demonstrated that a tumor of size 5 mm inside the glandular region could be located.

A fully automatic time-domain UWB unit named  $\chi - 1$  system was developed in 2018 by Shao et al. with a pair of movable antennas which could be independently rotated about a region of interest on their own track [121]. However, it was pointed out that the movement of the mechanical parts proved to be a disadvantage as it created artifacts. In 2019, Mukherjee et al. developed a time reversal based pulsed time-domain system (Fig. 4(c)) which could produce successful detection of single and multiple tumors that are embedded in a liquid breast tissue-based phantom [122]. Antipodal Vivaldi antenna was used as the fixed transmitter, and a monopole antenna was used as the receiver which was moved to mimic an antenna array. Yet another time-domain system was developed by Oloumi et al. in 2019 based on Circular SAR technique [123]. The microwave imaging results of MRI-derived 3D printed phantoms were superior to the output produced by MRI.

In spite of the differences in the front end, all of the above-mentioned time-domain systems depend on a high-precision pulse generator and very high-speed oscilloscope and require complicated switching circuits. To overcome this, researchers came up with fresh ideas of using CMOS-based circuitry. Kwon et al. [124] and Seo et al. [125] came up with alternative CMOS circuits for high-speed pulse generator and oscilloscope that drastically miniaturized the circuit dimensions to  $45 \text{ cm} \times 30 \text{ cm} \times 14.5 \text{ cm}$ . The time-domain systems, however, suffer from a low signal to noise ratio, because high frequency RF signal attenuates rapidly within the breast tissue. To overcome this, the signals have to be measured repeatedly and averaged to improve SNR.

Once the reflected signals from the target are collected by the various types of imaging systems, they have to be reconstructed using different focusing algorithms to detect/localize tumors.

### 3.2.2. Focusing Algorithms

Focusing algorithms are used to synchronize the signals collected during the data acquisition phase with respect to each breast focal point. They help to identify the positions of strong radiations that correspond to tumors. Focusing algorithms include Delay and Sum (DAS), Delay-Multiply And Sum (DMAS), Improved Delay-And-Sum (IDAS), Coherence Fator Based Delay-And-Sum (CFDAS), Channel Ranked Delay-And-Sum (CRDAS), Microwave Imaging via Space-Time (MIST), Multiple

Signal Classification (MUSIC), Weighted Capon Beamforming (WCB), Robust Weighted Capon Beamforming (RWCB), Generalized Likelihood Ratio Test (GLRT), etc.

DAS is a simple and robust method in which the signals are shifted by time 'T' calculated from the respective source locations relative to the antennas. DMAS is an improved version of DAS which performs a multiplication operation before the accumulation. The IDAS beamformer modifies the conventional DAS by introducing an additional weighting factor for each focal point, and this weighting factor is termed quality factor. In the CFDAS beamformer, a coherence based weighting factor is introduced in the conventional DAS algorithm which can enhance the coherence quality of radar signals. MIST beam-forming uses Finite Impulse Response (FIR) filters to compensate the frequency-dependent time delay, such as dispersion and fractional time delay [126]. MUSIC is a time reversal based algorithm. It is especially handy in cases of highly dense tissue background and helps to precisely focus at the target location [127]. But, the disadvantage is that the accuracy of imaging gets affected when the overall diameter of the tumor becomes less than 10 mm. MWI can also use a GLRT, which is a hypothesis-testing problem for each voxel, with the null hypothesis representing the tumor-free case [128]. All the above-mentioned focusing algorithms face performance degradation when being applied in dense breast situations. Hence they need to be combined with various clutter-removal algorithms [129, 130]. In addition, it is noted from various clinical trials that the average dielectric properties of breast tissues can vary substantially with density. This variation can impact both the image quality and sensitivity of imaging. In 2019, O'Loughlin et al. demonstrated the effectiveness of adopting parameter search algorithms to improve sensitivity of permittivity estimation techniques [131].

**Discussion:** Having discussed the principle of operation of various focusing algorithms, a comparison of these algorithms to identify the optimum method is necessary. Researchers from the McGill University in 2015 tried to compare four radar algorithms, i.e., DMAS, MIST, WCB, and GLRT on the data collected from healthy breast scans with injected tumor responses. The best sensitivity and specificity were shown by GLRT and DMAS algorithms with the GLRT classifier able to keep the false positive rate at 0.1 even while achieving a detection rate of 0.55 [132].

In 2017, research teams from University of Calgary and National University of Galway collaborated to compare the radar algorithms using data from TSAR imaging unit [133]. As a preliminary step, experimental phantoms (made of tissue mimicking materials) were imaged, and reconstruction performance of DAS, IDAS, DMAS, CFDAS, CRDAS and RWCB were compared. Signal to Clutter Ratio (SCR), Signal to Mean Ratio (SMR), and localisation error were selected as the comparison metric. DMAS was the only algorithm that significantly improved the image quality in terms of both SMR and SCR while keeping localization error within prescribed limits [162]. In 2018, these six algorithms were compared using actual clinical data [134]. The basic DAS algorithm was noted to be able to detect most malignancies, but the clutter level was significantly high. IDAS and CF-DAS reported the highest SMR and hence reduced clutter levels; however, the responses often did not correspond to the actual lesion locations from clinical reports. CR-DAS and RCB performed poorly across all patients. DMAS showed the second highest SMR with an improvement of 44% in comparison to DAS and comparable clutter suppression to IDAS. DMAS also ranked the best in terms of localisation of growths.

The above-mentioned comparison studies were carried out without considering the inter-patient variations in breast dielectric properties. Hence, in 2019 O'Loughlin et al. tried to assess the impact of patient-specific permittivity estimation on beamformer comparison and found that DMAS can "improve" both healthy and abnormal images [135].

From the results reported by various research teams who compared the various focusing algorithms in radar imaging, DMAS is noted to have the most balanced performance and may be suggested as a suitable choice for future research efforts in this domain [132–135].

### 3.3. Holographic Imaging

Holographic Imaging is derived from the hologram technique in optics. This technique was introduced into microwave imaging by Leith and Upatneiks [136]. Holographic techniques were taken by researchers due the simplicity in implementation. Holographic imaging proceeds in a two step process. The first step involves recording a holographic interference pattern (hologram) by illuminating the object under study from the source, called recording step. The second step deals with the reconstruction of the object from

the hologram with the help of a reference signal, named the reconstruction step. Holographic imaging proceeded in two directions, namely, direct holography and indirect holography.

Direct holographic imaging uses two different signals, one for the illumination of the object under study and the other as the reference signal, with both signals usually being of two different frequencies [137]. Majority of the holography-based breast tumor detection systems are based on direct holography, and they make use of VNA to record both the magnitude and phase of the back-scattered waves directly in an aperture. They are found to be similar to Synthetic Aperture Radar (SAR) techniques [138].

Amineh et al. tried to extend this technique into near-field imaging [139]. Since the analytical approximations of the incident field and the Green's function in the near-field were inadequate, effective experimental techniques were developed to quantify these parameters [140]. This approach proved to be a fast and robust means to reconstruct qualitative images of the imaged objects. In 2018, to avoid the wideband imaging and its complexities (time, cost and bulkiness), this method was extended to a single-frequency approach [141]. Again in 2018, Wang and Fatemi took an effort to incorporate compressive sensing into holography. CS techniques of Split Bregman (SB) and Orthogonal Matching Pursuit (OMP) were employed for the reconstruction of the experimentally collected scattered data to detect arbitrarily-shaped small inclusions by using significantly fewer sensors [142].

Indirect holography uses a reference signal that is generated from the same source as the illumination signal. The output from the microwave generator is split by a directional coupler to provide one signal to illuminate the object under investigation and a second signal to form the reference signal. It is based on the Synthesized Reference Beam method [143]. Indirect holography offers a simple and inexpensive technique for the determination of complex scattered fields using only scalar intensity measurements taken over a single aperture. Such an arrangement also does not require the use of costly equipment like VNA and can be performed using basic power measuring devices like square law detector [138]. In the arrangement used by Smith et al., the field scattered by the object is applied to one of the inputs of the hybrid tee, while the other input is fed with the reference signal. The combined signal is processed using Fourier transform for tumor detection [144, 145].

On the whole, it can be seen that since holography uses a direct inversion procedure, the method is fast and can perform in quasi-real time [141]. However, holographic MWI has certain drawbacks. Holography is based on a linearized scattering model which does not take into account the effects of multiple scattering or the nonlinear relation between the scattered field and target contrast [146]. Additionally, the level of reconstruction accuracy offered by holographic imaging is also low.

### 3.4. Hybrid Imaging

Along the course of development of MWI systems, some researchers attempted to develop hybrid techniques to compensate the handicaps of one imaging modality by the strength of another. Many breast cancer studies reported marked improvement in diagnostic performance when data from one modality were clubbed with another [147]. Mainly, MWI hybrid systems include microwave-acoustic imaging units, MWI-MRI hybrid units, MWI-mammogram hybrid units, etc.

Hybrid microwave acoustic imaging works on the principle that malignant tissues have higher conductivity properties than healthy cells and hence absorb more microwave energy. Thus, the excited tumor cells expand and generate acoustic/pressure waves which are then sensed by ultrasound sensors placed around the breast. Basically, there are two types of microwave-acoustic imaging: Computed thermo-acoustic tomography and Scanning thermo-acoustic tomography.

Computed thermo-acoustic tomography is named so because it uses an adapted version of reconstruction used in CT-scan imaging (filtered back projection algorithm) [148]. Kruger et al. were the pioneers of this approach. Microwave pulses at 434 MHz were applied to the breast, and the resulting signals were collected by a hemispherical array of 64 ultrasound transducers [149]. Many improvisations of the basic back propagation algorithm have been reported like the real time Radon transform-based algorithm [150] by Zanger et al., modified back-propagation algorithm by Xu et al. [151], etc. Ye et al. developed a real-time imaging setup with an ultra-short microwave pulse generator and a ring transducer array with 384 elements [152]. Successful imaging of an ewe breast was carried out by the team which is to be extended towards human clinical trials as the next step.

Scanning thermoacoustic tomography was initiated by Xu et al. They used microwave signals in the Gigahertz range for illumination and used stacking of the time-domain data collected by ultrasound transducers for image formation [153]. Abbhosh developed a hybrid system with dual excitation (microwave + acoustic). While microwaves imaged the dielectric contrasts, acoustic signals provided a full view of the elasticity distributions within the breast. These two distributions were combined to produce a final image with high contrast and resolution [154].

Microwave-MRI hybrid systems were developed as it was observed that higher water density in tumor tissues can obscure the visibility and hence the detection of tumor in MRI. An MWI system incorporated within an MRI scanner was materialized by Golnabi et al. (Fig. 5(a)) in 2016 [155] which was also patented (Patent No. US 8,977,340 B2). In 2019, the team reported that the incorporation of structural priors derived from MRI increased the contrast between tumor and fibroglandular tissue by 59% in permittivity and 192% in conductivity [156].

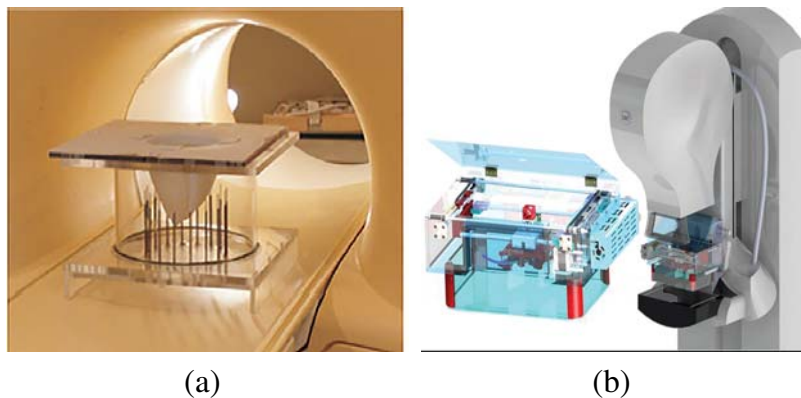


**Figure 5.** Hybrid systems developed by (a) Golnabi et al. [156] and (b) Dagheyan et al. [157].

Figure 5(b) depicts the arrangement of a hi-tech setup combining MWI and mammography [157]. The system employed antipodal Vivaldi antennas to overcome the limitations of band-limited Vivaldi antennas and applied Born approximation to reconstruct high quality images. The system is reported to be ready to move into clinical trials. Near-field MWI has the potential to alleviate the problem of low contrast faced at X-ray frequencies as tissues show more contrast at microwave frequencies [157].

In an MWI-US system, ultrasound information is incorporated into the MWI inversion process so that the combined information obtained from both the systems can help build a more complete diagnostic tool. Jiang et al. developed a multi-modality approach in which microwave image reconstruction is structurally guided by ultrasound imaging [158].

In hybrid systems although the disadvantages of one modality is compensated by the other, certain open issues exist as mentioned below.

- In computed thermo-acoustic tomography, the radiated microwave energy is relatively weak due to large radiation area. Also, since the microwave frequency used is low of only 434 MHz, the microwave absorption coefficients are relatively low. These two factors result in a low signal to noise ratio and also make the contrast low. To solve this problem if we increase the frequency, the microwave absorption coefficients are improved, and therefore the imaging contrast is also better. However, higher absorption leads to lower penetration depth [152]. In the future, such systems must develop a trade-off so that a more suitable operating frequency must be chosen that can balance the contrast and penetration depth.
- In an MWI-MRI system, the synchronized functioning of two modalities based on entirely different principles is a challenge demanding patience, skill, and continued effort. Hence, imaging is usually performed in separate sessions for each modality without disturbing another [155].
- When an MWI unit is placed in an MRI bore, interference of the magnetic fields occurs with the metallic part of the microwave imaging system [156].

- It is noted that the increase in hardware complexity is a major concern that hinders the research interest towards developing MWI-MRI/MWI-mammogram systems [157].

The major classes of MWI techniques including their imaging setups and reconstruction algorithms were discussed in this section. The major research efforts that have progressed into clinical trials and clinical practice will be discussed in the coming section.

#### 4. STATE-OF-THE-ART IN MWI

MWI has received contributions from researchers around the globe for the past 30 years or more. However, till 2019 MWI had been in the clinical trial phase. The results of these trials are summarized in Table 1. But now, MWI is rapidly transitioning into the clinical acceptance phase and actual clinical practice. After years of anticipation, the first steps of MWI into actual clinical imaging of the breast were initiated in 2019 with the introduction of MARIA breast tumor screening unit (seen in Fig. 6(a)) into hospitals in Germany. The novel MARIA system designed by the Bristol University and commercially developed by Micrima Ltd. has been installed in hospitals in Austria and Switzerland by Hologic Inc. (a global leader in woman health) [31]. Hologic chose the German Rontgen Congress held in June 2019 for the first unveiling of the MARIA system to their customers.

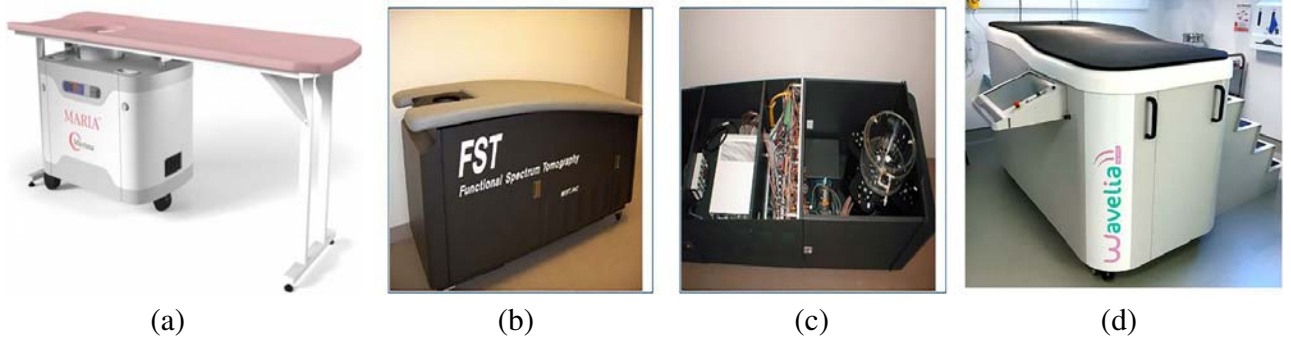


**Figure 6.** (a) MARIA unit [31], (b) unit at Dartmouth College [161] and (c) Wavelia [167].

**Table 1.** Summary of microwave breast imaging systems.

	Patients	Position	Technique	Freq (GHz)	Antenna	Scan time
Bristol University, UK	223	prone	Radar	3–8	slot	30 s
Dartmouth College, USA	150	prone	Tomo	0.7–1.7	monopole	5 min
ETRI, Korea	15	prone	Tomo	3–6	monopole	15 s/slice
MU (table)	13	prone	Radar	2–4	TWTLTLA	18 min
MU (wearable)	38	wearable	Radar	2–4	microstrip	5 min
SUC, China	11	prone	Radar	4–8	horn	4 min
TSAR, Canada	8	prone	Radar	1.3–7.6	vivaldi	30 min
HU, Japan	5	supine	Radar	3.1–10.6	planar slot	3 min
SU, Japan	2	prone	Radar, tomo	4–9	stack patch	3 min
Microwave Vision	pilot	prone	Radar	1–4	Vivaldi	10 min
Mammowave, Italy	51	prone	HP	1–9	PulsON P200	10 min
Kobe University, Japan	20	supine	tomo	0.05–12	UWB	30 min

The total scanning time of a breast for MARIA system is less than 1 minute with image generation taking less than 5 minutes [31]. The most remarkable feature of MARIA is its exceptional sensitivity in dense breast cases. In the clinical trial results published in 2017 (shown in Table 1), MARIA was

able to attain 86% sensitivity for dense breast cases while maintaining an overall sensitivity of 75% (i.e., 60/80 patients; age 32–89) [159, 160]. In the last quarter of 2019, Micrima appointed leading scientists in artificial intelligence to accelerate its product development [31].

Two other commercial ventures for breast tumor detection were made by the Microwave Imaging System Technologies-MIST (Dartmouth College, USA) and Microwave Vision SA, France.

Dartmouth College researchers led by Meaney et al. were the initial contributors to MWI. MIST was founded in 1995 by Dr. Keith Paulsen and Dr. Paul Meaney of the Thayer School of Engineering, Dartmouth. Fig. 6(b) shows the imaging unit developed by the group and its interior structure. Inspired by the results from initial clinical trials, tumor detection was extended towards tumor monitoring. Monitoring involved assessing the progress/regress in tumor growths by the exposure to neoadjuvant chemotherapy through MWI [161]. The study results showed that conductivity had a higher correlation with tumor presence than the corresponding permittivity values. Moreover, it was also reported that the normalized conductivity readings taken 30 days after the beginning of treatment had good correlation with tumor response. Various efforts were taken by MIST researchers to address some of the more practical issues faced by the imaging system and to improve the performance. Suppressing unwanted multi-path signals was attained by providing a lossy coupling bath and using high gain-monopole antennas [162]. The group was also able to patent a method that used a precious metal nanoparticle contrast agent for microwave imaging [163]. Contrast agent used was gold nanoparticle that could enhance the dielectric contrast between malignant and fibrous tissues. In 2019, Discrete Dipole Approximation (DDA) was developed for efficiently calculating the two-dimensional electric field distribution which helps to accelerate the forward problem computations [164]. In 2019, efforts were also made to replace the VNA for the first time in tomography by developing a 4-channel VNA based on software defined radio technology [165]. The inherent disadvantages of SDR technology like limited dynamic range and unreliable coherence between multiple boards were overcome by using low noise amplifier and other external microwave circuitry.

Microwave Vision group developed the Wavelia imaging system (Fig. 6(c)) for robust breast tumor detection [166]. The device installed at Galway University hospital took approximately 10 minutes to complete a scan [167]. After an on-site validation, efforts were made to identify and mitigate possible sources of measurement uncertainty due to the contributions of the thermal environment, mechanical movements, and system noise floor [168]. Now the group is engaged in active clinical trials with 30 tumor patients whose results are expected by the end of 2020 [169]. One more table-based arrangement was brought about by ETRI in Korea [170]. A unique fast electromagnetic solver performed non-blind imaging of 15 women, and the reconstructed images were validated against mammogram by radiologists from Seoul National University Hospital. 28 images out of the total 30 images coincided with medical analysis, and 2 cases were different (false negative-1 and false positive-1). A Fast Forward electromagnetic Solver (FFS) was developed in 2017 to speed up the processing involved in the imaging unit [171]. In 2019, super-resolution effects were analysed for the imaging unit utilizing a truncated singular value decomposition-based approach in the linear (Born approximation) and nonlinear modeling in near-field zone [172]. It was also verified that nonlinear reconstruction produced a spatial resolution that can be remarkably smaller than that for the linear consideration.

McGill University (MU) developed a prone arrangement and a wearable prototype employing a 16-element antenna array for imaging (discussed in Section 3.2.1). A sample comprising 342 breast scans collected over an eight-month period with 13 healthy volunteers was reconstructed [173]. Later, in 2017, the collected clinical trial data were tested against three fusion strategies [174] to perform classification using cost-sensitive support vector machines. These algorithms were able to choose thresholds in a principled manner to ensure that the false positive rate remained low. In 2019, the team reported the results from a new set of clinical trials performed on 38 patients [175] whose mammogram or MRI had previously indicated an abnormality. For the purpose of the clinical study, the wearable prototype bra was embedded within an examination table. The study results showed statistically significant correlation between patient age and breast density, as well as between patient age and signal level.

The radar imaging system experimented-with by the researchers from Southern University of China (SUC) was used for mammary hyperplasia detection, with special focus on Asian women (11 patients). Hyperplasia is a benign overgrowth of the cells that line the ducts or the mammary glands. A patient diagnosed with hyperplasia has a higher chance of developing breast cancer in the near future than those

without such a growth [176]. It was observed that healthy volunteers presented much less scattering than the breasts with hyperplasia. Inspired by the positive results with hyperplasia, the group has extended the clinical trials for breast tumor detection with over 100 recruits.

Tissue Sensing Adaptive Radar (TSAR) developed by Calgary University is a sophisticated imaging unit employing only a single antenna with four degrees of freedom [177]. The results obtained from this system were found to match well with the clinical analysis [178]. Recently, the researchers used the imaging unit to compare the performance of various reconstruction algorithms on the data collected during imaging. From the analysis based on SNR, clutter suppression, localization error, etc., DMAS algorithm was identified to be the most suitable technique for reconstruction [132–134]. Shizuoka University (SU) also concentrated upon a table-type model with the antennas embedded in a cup manufactured by Sumitomo Electric Industries, Ltd., whose material has almost the same electromagnetic parameters as the adipose tissue [179]. The team completed the scattered signal acquisition using the radar-based unit, and the reconstruction was done by tomographic DBIM algorithm. Prior information made available by radar imaging complemented the reconstruction quality of the tomographic inversion process.

Hiroshima University (HU) developed a portable handheld model against the widely used table-top design. The designed unit measured mere  $19.1\text{ cm} \times 17.7\text{ cm} \times 18.8\text{ cm}$  making it a very useful tool for imaging [180]. Further on, in 2018, the portable detector was modified to produce a reduced scan time of merely three minutes from the earlier 15 minutes when the antenna array rotated in steps of 15 degrees [181]. This system could visualize breast tumors with a diameter of 1 cm or more. Results from this clinical study indicated that the impulse-radar detector had two advantages. First, it detected a breast cancer that could not be recognized via mammography in a patient with heterogeneous dense breast. Second, the device also detected a micro-invasive carcinoma with an invasive tumor size of 0.5 mm. The SP8T switch [182] used in the above study was first upgraded to DP4T switch in 2018 and later to a DP8T switch in 2019 with improved insertion loss, bandwidth, and isolation [183, 184]. The research team also developed a Gaussian monocycle pulse generator calibration circuitry to enhance the detection accuracy [185].

The Mammowave device developed by Sani et al. based on the Huygens Principle is equipped to detect and localize tumors [186]. The device was employed to image 22 healthy patients and 29 patients with abnormalities. The team reported a true positive rate of 0.7 and false negative rate of 0.35 [187]. Researchers from Kobe University led by Kenjiro Kimura have developed a novel device for 3D-microwave mammography [188]. Accurate detection has been made in over 300 patients screened to have tumors through MRI or mammogram. The team has developed the device on the principles of inverse scattering patented under US 2016/0377557 A1 and EP2957925B1 [189, 190]. Clinical trials are progressing in 20 patients, and the device is expected to be commercially available by 2021.

This section discussed the results reported by the major research groups engaged in clinical trials which are rapidly moving into practical imaging scenario around the globe. As against the simulation environment, practical imaging scenarios posed many challenges before the researchers. These concerns observed during clinical trials and their plausible solutions are discussed in the forthcoming section.

## 5. CONCERNS OBSERVED DURING CLINICAL TRIALS AND THE POSSIBLE SOLUTIONS

Clinical trials brought to light the shortcomings of MWI in patient positioning, scan duration, coupling efficiency, contrast issues, marketing strategy, etc. which need to be addressed before it can be put to actual clinical practice.

### 5.0.1. Patient Positioning and Scan Duration

Prone positioning of the patient is the most accepted position among researchers as the hanging breast provides easy access to the entire breast and avoids the uncomfortable compression as in mammography. But from the numerous clinical trials conducted, it was observed that it was difficult to image the growths in the axilla region or those bordering chest walls. Another disadvantage with prone systems is that lying still in the prone position during the entire scan duration is hard for patients especially in

advanced cancer stages thereby necessitating reduced scan times. Supine or sitting positioning offered by wearable prototypes is a decent option that can provide a comfortable imaging session for the patient. However, the disadvantage in wearable systems is that the prototype will have a fixed cup size for breast placement. This leads to incomplete coverage in cases of patients with large breast sizes and gaps in cases of small breast sizes.

#### *5.0.2. Coupling Efficiency*

Since the electrical property difference between the body and the imaging system is high, strong reflection occurs at the tissue boundary. Thus, a suitable coupling mechanism is needed to ensure that microwave signals are effectively transferred into the imaged organ. A common technique adopted in table-type arrangements is to keep the breast immersed in a low-loss coupling medium like corn syrup, sodium metasilicate gel, etc. [191]. But the enhancement in the extent of coupling comes at the cost of many practical inconveniences. Immersion-based systems are prone to patient movement during scans. Additionally, disinfecting the tank to ensure hygiene by emptying its contents after each scan is expensive and time consuming. To do away with the disadvantages of coupling liquids, Amineh et al. proposed an antenna structure embedded in dielectric materials with properties closer to those of tissues [192]. Additionally, some radar-based models (MARIA, SU) started using coupling shells or radomes housing the antenna array at close proximity to the skin. This design could couple almost 90% of the microwave power into the tissues. Another preferred option is the use of a bio-compatible material for coupling shell design. The wearable systems do not need coupling liquids of any kind, but good contact is attained by having the bra to be a little undersized. Complete coverage of the entire breast may however be compromised in this effort.

#### *5.0.3. Low Contrast*

The actual contrast in permittivity obtained between fibroglandular tissue and cancerous growths is much lower than the contrast between adipose and malignant tissues. This low contrast is a major concern in patients with dense breasts. But the results from the experiments conducted with the new version of MARIA (employing a ceramic cup lined with a small amount of contact fluid of dielectric constant 10) exhibiting a high sensitivity of 86% in dense breast cases have raised hopes for definiteness in detection. Several researchers also came up with the idea of nanomaterial contrast agents like microbubbles, carbon nanotubes, etc. to enhance the permittivity differences [193]. These contrast agents are reported to be able to provide an increase of 37% in dielectric permittivity and 81% in conductivity of tumor without changing the electrical properties of other tissues [194]. Magnetic Nano-Particles (MNP) [195, 196] which are widely used in biomedical applications was suggested by Bucci et al. which made use of differential scattering under the effect of magnetic field to enhance detection [197, 198]. Researchers from the Dartmouth College patented the technique of contrast-enhanced imaging using gold nanomaterial [163]. In 2019, Akinici et al. employed carbon nanotubes and a factorization-based reconstruction algorithm to obtain qualitative imaging [199].

#### *5.0.4. Choice of Domain and Imaging Technique*

Tomographic, radar, and holography based imaging techniques and their hybrid versions are the options at hand. Tomography provides complete information but at the cost of increased computational burden and duration of scan. Recently, the substitutes for the costly switching networks in tomographic imaging based on PIN diodes or circulators have been proposed [200]. The frequency domain radar techniques which needed bulky and costly equipment can now be replaced with FPGA-based models [118]. Time-domain radar systems have also come up with miniaturized circuits using CMOS designs [124, 125]. Miniaturized SDR-based VNA is being developed widely by many prominent research groups [116, 196]. However detection and localization alone is made possible in radar-based systems. Holographic systems have a fast implementation and apply a direct inversion process; however, it is based on a linear scattering model which can lead to inaccurate reconstruction results. The right choice must be made depending upon the resources at hand. Radar imaging that uses a simpler and hence faster

reconstruction process and produces accurate tumor detection may be suggested as a feasible option for regular screening.

#### 5.0.5. Current Market Scenario

Microwave imaging is a breakthrough technology among the safe methods of biomedical imaging. However, this technique has not been fully bought by the industrial domain owing to the competition from other modalities such as MRI, CT scan, etc. Establishments like Micrima, MIST, Microwave Vision SA, etc. are a few of the commercial players in this field [31, 162, 167]. Apart from the technical hardships, financial investments are also hindering the transition of MWI into a real life imaging technique. Large investments are needed to carry out large scale studies to determine the problems in the applied techniques and to refine them, for acquiring high computational facilities, for procuring high-end equipments like VNA's, high speed switching networks, etc.

## 6. OPEN CHALLENGES FACED BY MWI AND FUTURE PROSPECTS

There are a lot of factors that hinder the development of MWI with such immense potential from entering the practical imaging scenario. Such gap areas and some suggestions to tackle these issues are discussed here.

- Device portability: It is always desirable for imaging systems to be portable. Portable MWI units can be brought to the cancer-affected patients' bed-side for the monitoring of malignant growths. Wu and Amineh have reported a low-cost and portable imaging unit capable of producing 3D reconstruction through near-field imaging [201]. Furthermore, Hiroshima University developed their portable breast screening unit with an aim to be useful in cases of natural disasters and other calamities [180]. SDR based network analyser [116, 165], FPGA-based [118] and CMOS-based radar circuitry [124, 125], and PIN-diode based switching networks [200] are the possible directions that may be taken to achieve this aim.
- Optimum frequency: MWI researchers are yet to reach a consensus on the optimum frequency range for imaging to be carried out. It is a well-known fact that as the frequency increases, the resolution becomes better, but the penetration into tissues is seriously affected. This is because the penetration losses in tissues go up with frequency. Since the penetration loss of healthy fat tissue is less than 4 dB/cm with microwave signal which is centered at 6 GHz, frequency bands within the UWB frequency range is appropriate for near-field breast imaging [2].
- 3D modeling: 3D modeling helps to model the actual scenario more closely than 2D modeling which gives information only about a single cross section of the complete imaging volume. 2D modelling also uses many approximations to arrive at the reconstructed profile. For instance, when cylindrical phantoms are employed in 2D studies, for any cross-section, it is actually required that the height of such cylinders ideally are infinitely large for the approximations used in modeling to be applicable. Such heights, however, are not feasible for practical implementation. Phantoms of finite heights will affect the accuracy of the results obtained as it leads to imperfect modeling and inaccurate reconstruction results. 3D modeling must hence be taken by researchers involved in the modeling studies as it avoids such ambiguities and can help them to move on into phantom studies and handle spherical/hemispherical/arbitrary shaped breast phantoms accurately.
- Number of antennas: Increasing the number of antennas in the sensor array is another option to increase the amount of data-at-hand. This, however, increases the mutual coupling among antennas and will make the inverse problem more complex. Hence, a compromise has to be reached between these two factors. There is an upper limit on the number of antennas that can be placed in an MWI scattering setup as set by the degrees of freedom theory [202]. The upper bound on the collectible information is determined by the degrees of freedom involved which is practically equal to the Nyquist number and is proportional to the spatial bandwidth of the field and the extent of the observation domain [203].
- Inverse profiling: The inversion algorithms must be fine-tuned according to the acquisition device involved and made highly accurate. For tomography-based systems, DBIM or Gauss Newton

algorithms may be combined with a greedy CS technique (e.g., Subspace Pursuit) to achieve quality reconstructions. Expansion-based representations like wavelet, cosine spline, cosine Fourier, Fourier Jacobi, etc. are useful tools. In radar imaging, DMAS algorithm is seen to be the most effective.

- Researchers must also strive for developing entirely new inverse profiling strategies which are highly robust and efficient especially in dense breast cases.
- Frequency hopping: It is a technique that employs multiple frequencies for better reconstruction [204]. It overcomes the effect of non-linearity in the optimization procedure so that an algorithm does not get trapped in local minima as shown by Salucci et al. [205]. An improvisation to the sequential implementation of the frequency hopping can be obtained through the multiresolution technique which can iteratively zoom on the detected region-of-interest to adaptively improve the resolution of the retrieved image. This process allows one to keep the number of pixels within the background region low, thus mitigating the occurrence of local minima in the cost function [80].
- Sparsity issues: Converting the scattered signal data into a sparse form is not always feasible. Hence, systems that can generate sparse data are to be designed. Moreover, acquiring a priori knowledge about the target may not be always possible. Therefore, robust CS strategies that can work without any a priori data (e.g., color CS) are needed [94].
- Large-scale trials: The studies undertaken by various research groups have to be immediately extended into large-scale clinical trials to perfect the glitches in the imaging devices and algorithms. Such trials can help in correctly judging the efficiency of the unit to be versatile in imaging patients belonging to various ethnic groups, races, patients with varying tissue densities, etc.
- Service to society: All research efforts towards tumor/stroke detection must be taken on a humanitarian concern and not for financial or professional gain. A coordinated effort by pooling in the information and expertise of different teams could aid in a faster and technologically advanced model at a reduced cost. Sensitivity, specificity, accuracy level of reconstruction, etc. must be documented and reported authentically to assess the actual progress made by various research groups in this domain.
- Industrial involvement: The abundant potential possessed by MWI in light of the results of the trials must be rightly communicated with the industry and more commercial firms, especially start-up ventures must be drawn into this effort to ensure that more ready-to-use MWI systems are made available in the immediate future.
- Financial crunch: is a major setback faced by all researchers in the MWI field. Government agencies and university departments must be invoked to provide funds to promote the development of this modality since it can be a great improvement to the current medical imaging standards as a safe, robust, and affordable technique.
- Deep learning: Deep learning neural networks applying paradigms, such as machine learning and dictionary learning, must be taken up in future to speed up the inversion process [206]. In the past few years, improved regularization schemes and compressive sensing techniques have been adopted to approach the highly ill-posed inverse problem. However, when the scattering is strong, the problem becomes highly non-convex, which negatively impacts both the speed of reconstruction and the quality of the final image. Hence, researchers have started placing the multiple scattering data as the forward-pass of a Convolutional Neural Network (CNN or ConvNet) [207]. CNN deep learning algorithm works with neurons that have learnable weights and biases. They combine the extracted features and aggregate them in a nonlinear fashion to predict the output [208]. CNN-based learning is more efficient because it reduces the number of parameters. The reduction is possible because it takes advantage of feature locality. They work by learning low level or meaningless features in their first layers and then stack them so as to have a meaning in the higher layers. When deep learning is applied to inverse problems, the technique tries to reconstruct the object by designing a CNN that is specifically trained to invert multiple scattering in a purely data-driven fashion [209]. CNN's with only the last layer having a connected structure can work much faster than traditional neural networks and reduce the computational burden faced in inverse scattering problems. Some of the latest works have already reported the various deep learning paradigms to help simplify the complex inverse problem [210–213]. Moreover, Micrima and EMTensor teams have already engaged in improvising their clinical models using deep learning.

- A significant milestone towards handheld MWI units has been reached with the development of a chip-based microwave optical near-field imager by researchers from Pennsylvania University [214]. The chip with a size of  $2\text{ mm} \times 2\text{ mm}$  will help to do away with the conventional bench-type systems. In this chip, the impinging microwave signals are upconverted to the optical domain and optically delayed and processed to form the near-field image of the target object.

## 7. CONCLUSION

MWI is a microwave-based imaging modality that is safe, non-ionizing, and non-invasive in nature. Hence, MWI-researchers are striving hard to introduce this useful technology into practical imaging scenario. In several situations, the contrast in dielectric values was seen to reach a low of even 10% owing to the fibroglandular tissues which differ only slightly from cancerous tissue in permittivity. But, this low contrast is only a worst case scenario faced by MWI, and latest research results have proved that even with this small permittivity difference quality detection is possible.

Imaging using microwaves can be carried out using tomography, radar-based imaging, holography, or the hybrid versions of these methods. To attain improved results, MWI researchers can make use of the immense possibilities offered by deep learning paradigms implemented using CNN framework. Deep learning reduces the number of parameters handled in the inverse problem by using layered learning by employing neurons that are assigned learnable weights and biases. Deep learning techniques may be coupled with frequency hopping and multi-resolution methods to increase the execution speed manifold.

In spite of its immense potential, MWI was able to move into clinical trials only in the past few years. Many MWI prototypes are presently engaged in active clinical trials to counter the shortcomings observed during practical scenarios and rectify them. Industrial involvement has been initiated by Micrima, MIST, Medfield diagnostics, etc. in commercializing the MWI technology. After many years of clinical trials, a major milestone towards the transition of MWI into active clinical imaging was achieved recently. The MARIA breast tumor screening system (commercially developed by Micrima, UK) has been installed in hospitals in Germany which is soon to be followed by hospitals in Austria and Switzerland. It is hoped that the pitfalls observed by other research groups in their imaging systems are soon corrected. Hence many more MWI imaging systems can enter into practical imaging scenario allowing for microwave imaging to become a full-fledged biomedical imaging modality in the near future.

## REFERENCES

1. Jamali, N. H., K. A. Hong Ping, S. Sahrani, and T. Takenaka, "Image reconstruction based on combination of inverse scattering technique and total variation regularization method," *Indonesian J. Electrical Engineering and Computer Science*, Vol. 5, 569–576, 2017.
2. Kwon, S. and S. Lee, "Recent advances in microwave imaging for breast cancer detection," *Int. J. Biomed. Imaging*, Vol. 206, 1–26, 2016.
3. American Cancer Society, Cancer Facts & Figures 2019, <https://www.cancer.org/cancer/breast-cancer/about/how-common-is-breast-cancer.html>, accessed Mar. 2019.
4. Fear, E. C., "Confocal microwave imaging for breast cancer detection: Localization of tumors in three dimensions," *IEEE Trans. Biomed. Engineering*, Vol. 49, 812–822, 2002.
5. Guo, R., G. Lu, and B. Fei, "Ultrasound imaging technologies for breast cancer detection and management — A review," *Ultrasound Med. Biol.*, Vol. 44, 37–70, 2018.
6. Bowles, D., et al., "The use of ultrasound in breast cancer screening of asymptomatic women with dense breast tissue: A narrative review," *Journal of Medical Imaging and Radiation Sciences*, Vol. 47, 21–28, 2016.
7. Vitual Medical Centre, PET Scan (Positron Emission Tomography), <https://www.myvmc.com/investigations/pet-scan-positron-emission-tomography.html>, accessed Nov. 2019.
8. Schueren, M. V., "Safety assessment of microwave radar breast imaging in the 0.434–9 GHz range," Master Thesis, Department of Electrical & Computer Engineering, McGill University Montreal, Quebec, Canada, Jun. 2011.

9. Rezaeieh, S. A., "Wideband microwave imaging systems for the diagnosis of fluid accumulation in the human torso," Ph.D. Thesis, University of Queensland, Australia, 2016.
10. Cleveland, R. F. and J. L. Ulcek, "Questions and answers about biological effects and potential hazards of radiofrequency electromagnetic fields," *OET Bull.*, Vol. 56, 1–36, 1999.
11. ICNIRP Guidelines, "Guidelines for limiting exposure to time-varying electric, 6 magnetic and electromagnetic fields," 2018.
12. Larsen, L. E. and J. H. Jacobi, *Medical Application of Microwave Imaging*, 229, IEEE Press, New York, 1986.
13. Grzegorzczuk, T. M., P. M. Meaney, P. A. Kaufman, R. M. Di Florio-Alexander, and K. D. Paulsen, "Fast 3-D tomographic microwave imaging for breast cancer detection," *IEEE Trans. Medical Imaging*, Vol. 31, 1584–1592, 2012.
14. Elahi, M. A., B. R. Lavoie, E. Porter, M. Glavin, E. Jones, and E. C. Fear, "Comparison of radar-based microwave imaging algorithms applied to experimental breast phantoms," *Proc. URSI General Assembly and Scientific Symposium (GASS)*, Montreal, Canada, Aug. 2017.
15. Semenov, S. Y. and D. R. Corfield, "Microwave tomography for brain imaging: Feasibility assessment for stroke detection," *Int. J. Antennas Propag.*, 1–8, 2008.
16. Scapatucci, R., L. Di Donato, I. Catapano, and L. A. Crocco, "Feasibility study on microwave imaging for brain stroke monitoring," *Progress In Electromagnetics Research B*, Vol. 40, 305–324, 2012.
17. Dogu, S., I. Dilman, M. C. Joren, and I. Akduman, "Imaging of pulmonary edema with microwaves-preliminary investigation," *Proc. International Conference on Electrical and Electronics Engineering (ELECO)*, Bursa, Turkey, 2017.
18. Ghavami, N., G. Tiberi, M. Ghavami, and M. Lane, "Huygens principle based UWB microwave imaging method for skin cancer detection," *Proc. International Symposium on Communication Systems, Networks and Digital Signal Processing (CSNDSP)*, Prague, Czech Republic, 2016.
19. Mobashsher, A. T. and A. Abbosh, "Microwave imaging system to provide portable-low powered medical facility for the detection of intracranial hemorrhage," *Proc. Australian Microwave Symposium (AMS)*, Melbourne, Australia, 2014.
20. Meaney, P. M., D. Goodwin, A. H. Golnabi, and K. D. Paulsen, "Clinical microwave tomographic imaging of the calcaneus: A first-in-human case study of two subjects," *IEEE Trans. Biomed. Engineering*, Vol. 59, 3304–3313, 2012.
21. Muqatash, S. A., M. Khamechi, and A. Sabouni, "Detection of the cervical spondylotic myelopathy using noninvasive microwave imaging technique," *IEEE Int. Symp. Ant. Propag. and USNC/URSI National Radio Science Meeting*, San Diego, USA, 2017.
22. Colton, D. and P. Monk, "The detection and monitoring of leukemia using electromagnetic waves: Numerical analysis," *Inverse Problems — IOPScience*, Vol. 11, 329–341, 1995.
23. Lin, J. C. and M. J. Clarke, "Microwave imaging of cerebral edema," *Proc. IEEE*, Vol. 70, 523–524, 1982.
24. Zamani, A., S. A. Rezaeieh, and A. M. Abbosh, "Lung cancer detection using frequency domain microwave imaging," *Electronics Lett.*, Vol. 51, 740–741, 2015.
25. Brovoll, S., et al., "Time-lapse imaging of human heartbeats using UWB radar," *Proc. Biomedical Circuits and Systems (BIOCAS)*, Rotterdam, Netherlands, 2013.
26. Salvador, S. M., S. M. Fear, E. C. Okoniewski, M. Matyas, and R. John, "Exploring joint tissues with microwave imaging," *IEEE Trans. on Microwave Theory and Tech.*, Vol. 58, 2307–2313, 2010.
27. Alirotehand, M. S. and A. Arbabian, "Microwave-induced thermo-acoustic imaging of subcutaneous vasculature with near-field RF excitation," *IEEE Trans. on Microwave Theory and Tech.*, Vol. 66, 577–588, 2018.
28. Bolomey, J. C., "Crossed viewpoints on microwave-based imaging for medical diagnosis: From genesis to earliest clinical outcomes," *The World of Applied Electromag.*, 369–414, Springer International Publishing, Switzerland, 2018.

29. Modiri, A., S. Goudreau, and K. Kiasaleh, "Review of breast screening: Toward clinical realization of microwave imaging," *Med. Phys.*, Vol. 44, 446–458, Dec. 2017.
30. O'Loughlin, D., M. O'Halloran, B. M. Moloney, M. Glavin, and E. Jones, "Microwave breast imaging: Clinical advances and remaining challenges," *IEEE Trans. Biomed. Engineering*, Vol. 65, 1–14, 2018.
31. Micrima-Maria Update, "Micrima enters into distribution agreement with Hologic for its novel breast imaging system MARIA June 2019," <https://micrima.com/micrima-newsletters/vol6>, accessed Jan. 2020.
32. Farugia, L., P. S. Wismayer, L. Z. Mangion, and C. V. Sammut, "Accurate in vivo dielectric properties of liver from 500 MHz to 40 GHz and their correlation to ex vivo measurements," *Electromagnetic Biology and Medicine*, 1–9, 2016.
33. Salahuddin, S., A. L. Gioia, M. A. Elahi, E. Porter, M. O'Halloran, and A. Shahzad, "Comparison of in-vivo and ex-vivo dielectric properties of biological tissues," *Proc. ICEAA*, 582–585, Verona, Italy, 2017.
34. Amin, B., M. A. Elahi, A. Shahzad, E. Porter, B. McDermott, and M. O'Halloran, "Dielectric properties of bones for the monitoring of osteoporosis," *Medical & Biological Engineering & Computing*, Vol. 57, 1–13, 2019.
35. Ridley, N., A. Iriarte, and L. Tsui, "Automatic labeling of lesions using radio frequency feature discrimination," *Proc. European Congress of Radiology Annual Meeting*, Vienna, Austria, 2017.
36. Chaudhary, S. S., R. K. Mishra, A. Swarupand, and J. M. Thomas, "Dielectric properties of normal and malignant human breast tissues at radiowave and microwave frequencies," *Indian Journal of Biochemistry and Biophysics*, Vol. 21, 76–79, 1984.
37. Joines, W. T., Y. Zhang, and R. L. Jirtle, "The measured electrical properties of normal and malignant human tissues from 50 to 900 MHz," *Med. Phys.*, Vol. 21, 547–550, 1994.
38. Campbel, A. M. and D. V. Land, "Dielectric properties of female human breast tissue measured in vitro at 3.2 GHz," *Phys. Med. Biol.*, Vol. 3, 193–210, 1992.
39. Hurt, W. D., J. M. Ziriach, and P. A. Mason, "Variability in EMF permittivity values: Implications for SAR calculations," *IEEE Trans. Biomed. Engineering*, Vol. 47, 396–401, 2000.
40. Lazebnik, M., L. McCartney, and D. Popovic, "A large-scale study of the ultrawideband microwave dielectric properties of normal breast tissue obtained from reduction surgeries," *Physics in Medicine and Biology*, Vol. 52, 26–37, 2007.
41. Lazebnik, M., et al., "A large-scale study of the ultrawideband microwave dielectric properties of normal, benign and malignant breast tissues obtained from cancer surgeries," *Physics in Medicine and Biology*, Vol. 52, No. 20, 6093–6115, 2007.
42. Poplack, S. P., et al., "Electromagnetic breast imaging: Results of a pilot study in women with abnormal mammograms," *Radiology*, Vol. 243, 350–359, 2007.
43. Halter, R. J., et al., "The correlation of in vivo and ex vivo tissue dielectric properties to validate electromagnetic breast imaging: Initial clinical experience," *Institute of Physics and Engineering in Medicine*, Vol. 30, 121–136, 2009.
44. Chung, S. H., A. E. Cerussi, and A. Klifa, "In vivo water state measurements in breast cancer using broadband diffuse optical spectroscopy," *Phys. Med. Biol.*, Vol. 53, 6713–6727, 2008.
45. Shahzad, A., S. Khan, and M. Jones, "Investigation of the effect of dehydration on tissue dielectric properties in ex vivo measurements," *Biomedical Physics and Engineering Express*, Vol. 3, 1–9, 2017.
46. Meaney, P. M., A. P. Gregory, and N. R. Epstein, "Microwave open-ended coaxial dielectric probe: Interpretation of the sensing volume re-visited," *BMC Medical Physics*, Vol. 14, 1–11, 2014.
47. Meaney, P., T. Rydholm, and H. A. Brisby, "A transmission-based dielectric property probe for clinical applications," *Sensors*, Vol. 6, 1–16, 2018.
48. Gioia, A. L., S. Salahuddin, M. O'Halloran, and E. Porter, "Quantification of the sensing radius of a coaxial probe for accurate interpretation of heterogeneous tissue dielectric data," *IEEE J. Electromag. RF Microw. Medicine & Biol.*, Vol. 2, 1–9, 2018.

49. Porter, et al., "Minimum information for dielectric measurements of biological tissues (MINDER): A framework for repeatable and reusable data," *Int. J. RF Microw. Comput. Aided Eng.*, Vol. 28, 1–27, 2017.
50. Zubair, K. S., S. A. Alhuwaidi, H. H. Song, Y. G. Shellman, W. A. Robinson, A. J. Applegate, and C. M. Amato, "Investigation of dielectric spectroscopy response in normal and cancerous biological tissues using *S*-parameter measurements," *Journal of Electromagnetic Waves and Applications*, Vol. 32, No. 8, 956–971, 2018.
51. Hussein, M., F. Awwad, D. Jithin, E. Hasasna, K. Athamneh, and R. Iratni, "Breast cancer cells exhibits specific dielectric signature in vitro using the open-ended coaxial probe technique from 200 MHz to 13.6 GHz," *Scientific Reports*, Vol. 9, 1–8, 2019.
52. Gioia, L. A., et al., "Open-ended coaxial probe technique for dielectric measurement of biological tissues: Challenges and common practices," *Diagnostics*, Vol. 8, 1–38, 2018.
53. Slaney, M., A. C. Kak, and L. E. Larsen, "Limitations of imaging with first order diffraction tomography," *IEEE Trans. on Microwave Theory and Tech.*, Vol. 32, 860–874, 1984.
54. Semenov, S. Y., A. E. Boulyshev, and R. H. Svenson, "Three-dimensional microwave tomography experimental prototype of the system and vector Born reconstruction method," *IEEE Trans. Biomed. Engineering*, Vol. 46, 937–947, 1999.
55. Joisel, A., A. Broquetas, J. M. Griffin, L. Jofre, and J. C. Bolomey, "Microwave imaging techniques for biomedical application," *Proc. IEEE Instrum. Measure. Tech. Conference*, Venice, Italy, 1999.
56. Meaney, P. M., M. W. Fanning, and K. D. Paulsen, "A clinical prototype for active microwave imaging of the breast," *IEEE Trans. on Microwave Theory and Tech.*, Vol. 48, 1841–1853, 2000.
57. Son, S. H., N. Simonov, H. J. Kim, J. M. Lee, and S. I. Jeon, "Preclinical prototype development of a microwave tomography system for breast cancer detection," *ETRI Journal*, Vol. 32, No. 6, 901–910, 2010.
58. Zhurbenko, V., T. Rubaek, V. Krozer, and P. Meincke, "Design and realisation of a microwave three-dimensional imaging system with application to breast-cancer detection," *IET Microwaves, Antennas Propag.*, Vol. 4, 2200–2211, 2010.
59. Gibbins, D., D. Byrne, T. Henriksson, B. Monsalve, and I. J. Craddock, "Less becomes more for microwave imaging — Design and validation of an ultrawide-band measurement array," *IEEE Antennas Propag. Mag.*, Vol. 59, 72–85, 2017.
60. Fedeli, A., et al., "A tomograph prototype for quantitative microwave imaging: Preliminary experimental results," *J. Imaging*, Vol. 4, 1–9, 2018.
61. Zamani, A., S. A. Rezaeieh, K. S. Bialkowski, and A. M. Abbosh, "Boundary estimation of imaged object in microwave medical imaging using antenna resonant frequency shift," *IEEE Trans. Antennas and Propag.*, Vol. 66, 927–936, 2018.
62. Rezaeieh, S. A., A. Zamani, K. S. Bialkowski, G. M. Macdonald, and A. M. Abbosh, "Three-dimensional electromagnetic torso scanner," *Sensors*, Vol. 19, 1–14, 2019.
63. Asefi, M., A. Baran, and J. LoVetri, "An experimental phantom study for air-based quasi-resonant microwave breast imaging," *IEEE Trans. on Microwave Theory and Tech.*, Vol. 67, 3946–3954, 2019.
64. Joachimowitz, N., C. Pichot, and J. P. Hugonin, "Inverse scattering in iterative numerical method for electromagnetic imaging," *IEEE Trans. Antennas and Propag.*, Vol. 39, 1742–1752, 1991.
65. Chew, W. C. and Y. M. Wang, "Reconstruction of two-dimensional permittivity distribution using distorted Born iterative method," *IEEE Trans. Medical Imaging*, Vol. 9, 218–225, 1990.
66. Kishk, A. A., R. P. Parrikar, and A. Z. Elsherbeni, "Electromagnetic scattering from an eccentric multilayered circular cylinder," *IEEE Trans. Antennas and Propag.*, Vol. 40, 295–303, 1992.
67. Oliveri, G., N. Anselmi, and A. Massa, "Compressive sensing imaging of non-sparse 2D scatterers by a total-variation approach within the Born approximation," *IEEE Trans. Antennas and Propag.*, Vol. 62, 5157–5170, 2014.
68. Ireland, D., K. Bialkowski, and A. M. Abbosh, "Microwave imaging for brain stroke detection using Born iterative method," *IET Microw. Antennas Propag.*, Vol. 7, 909–915, 2013.

69. Burfeindt, M. J., J. D. Shea, and S. C. Hagness, "Beamforming-enhanced inverse scattering for microwave breast imaging," *IEEE Trans. Antennas and Propag.*, Vol. 62, 5126–5132, 2014.
70. Ye, X. and X. Chen, "Subspace-based distorted-Born iterative method for solving inverse scattering problems," *IEEE Trans. Antennas and Propag.*, Vol. 65, 7224–7232, 2017.
71. Neira, L. M., B. D. Van Veen, and S. C. Hagness, "High-resolution microwave breast imaging using a 3-D inverse scattering algorithm with a variable-strength spatial prior constraint," *IEEE Trans. Antennas and Propag.*, Vol. 65, 6002–6014, 2017.
72. Palmeri, R., M. T. Bevacqua, L. Crocco, T. Isernia, and L. Di Donato, "Microwave imaging via distorted iterated virtual experiments," *IEEE Trans. Antennas and Propag.*, Vol. 65, 1–9, 2016.
73. Meaney, P. M., S. D. Geimer, and K. D. Paulsen, "Two-step inversion with a logarithmic transformation for microwave breast imaging," *J. Medical Physics*, Vol. 44, 4239–4251, 2017.
74. Tournier, P. H., et al., "Microwave tomography for brain stroke imaging," *Proc. IEEE International Symposium on Antennas and Propagation & USNC/URSI National Radio Science Meeting*, San Diego, USA, 2017.
75. Bisio, I., et al., "Brain stroke microwave imaging by means of a Newton-conjugate-gradient method in  $L^p$  Banach spaces," *IEEE Trans. on Microwave Theory and Tech.*, Vol. 66, 3668–3682, 2018.
76. Autieri, R., G. Ferraiuolo, and V. Pascazio, "Bayesian regularization in nonlinear imaging: Reconstructions from experimental data in non-linearized microwave tomography," *IEEE Trans. Geosci. Remote Sens.*, Vol. 49, 801–813, 2011.
77. Rocca, P., M. Benedetti, M. Donelli, D. Franceschini, and A. Massa, "Evolutionary optimization as applied to inverse problems," *Inverse Prob.*, Vol. 25, 1–41, 2009.
78. Robinson, J. and Y. R. Samii, "Particle swarm optimization in electromagnetics," *IEEE Trans. Antennas and Propag.*, Vol. 52, 397–407, 2004.
79. Donelli, M., I. Craddock, D. Gibbins, and M. Sarafianou, "A three-dimensional time domain microwave imaging method for breast cancer detection based on an evolutionary algorithm," *Progress In Electromagnetics Research M*, Vol. 18, 179–195, 2011.
80. Salucci, M., L. Poli, N. Anselmi, and A. Massa, "Multifrequency particle swarm optimization for enhanced multiresolution GPR microwave imaging," *IEEE Trans. Geosci. Remote Sens.*, Vol. 55, 1305–1317, 2017.
81. Poli, L., G. Oliveri, and A. Massa, "Microwave imaging within the first-order Born approximation by means of contrast-field Bayesian compressive sensing," *IEEE Trans. Antennas and Propag.*, Vol. 60, 2865–2879, 2012.
82. Poli, L., G. Oliveri, P. Rocca, and A. Massa, "Bayesian compressive sensing approaches for the reconstruction of two-dimensional sparse scatterers under TE illuminations," *IEEE Trans. Geosci. Remote Sens.*, Vol. 51, 2920–2935, 2013.
83. Majobi, P. and J. LeVetri, "Comparison of TE and TM inversions in the framework of the Gauss-Newton method," *IEEE Trans. Antennas and Propag.*, Vol. 64, 1336–1348, 2010.
84. Shah, P. and U. K. Khankhoje, "Inverse scattering using a joint L1-L2 norm-based regularization," *IEEE Trans. Antennas and Propag.*, Vol. 64, 1373–1384, 2017.
85. Oliveri, G., M. Salucci, N. Anselmi, and A. Massa, "Compressive sensing as applied to inverse problems for imaging: Theory, applications, current trends, and open challenges," *IEEE Antennas Propag. Magazine*, Vol. 17, 34–46, 2017.
86. Candes, E. and J. Romberg, "l1-magic: Recovery of sparse signals via convex programming 2005," [http: www.acm.caltech.edu/l1magic/l1magicnotes.pdf](http://www.acm.caltech.edu/l1magic/l1magicnotes.pdf), accessed Jan. 2019.
87. Yalcin, E. and O. Ozdemir, "Sparsity based regularization for microwave imaging with NESTA algorithm," *Proc. IEEE Conference on Antennas Measurements and Applications (CAMA)*, Tsukuba, Japan, 2017.
88. Ambrosanio, M., P. Kosmas, and V. Pascazio, "A multithreshold iterative DBIM-based algorithm for the imaging of heterogeneous breast tissues," *IEEE Trans. Biomed. Engineering*, Vol. 66, 509–520, 2019.

89. Ambrosanio, M., M. Bevacqua, T. Isernia, and V. Pascazio, "The tomographic approach to ground-penetrating radar for underground exploration and monitoring," *IEEE Signal Processing Magazine*, Vol. 36, No. 4, 62–73, 2019.
90. Kosmas, P., et al., "Design and experimental validation of a multiple-frequency microwave tomography system employing the DBIM-TwIST algorithm," *Sensors*, Vol. 18, 1–13, 2018.
91. Kosmas, P., et al., "Experimental validation of microwave tomography with the DBIM-TwIST algorithm for brain stroke detection and classification," *Sensors*, Vol. 20, 1–16, 2020.
92. Zhou, H. and R. M. Narayan, "Microwave imaging of nonsparse object using dual-mesh method and iterative method," *IEEE Trans. Antennas and Propag.*, Vol. 67, 504–512, 2019.
93. Rudin, L. I. and S. Osher, "Total variation based image restoration with free local constraints," *Proc. International Conf. Image Processing*, Austin, USA, 1994.
94. Anselmi, N., G. Oliver, M. A. Hannan, M. Salucci, and A. Massa, "Color compressive sensing imaging of arbitrary-shaped scatterers," *IEEE Trans. on Microwave Theory and Tech.*, Vol. 65, 1986–1999, 2017.
95. Salucci, M., L. Poli, and G. Oliveri, "Full-vectorial 3D microwave imaging of sparse scatterers through a multi-task bayesian compressive sensing approach," *J. Imaging*, Vol. 5, 1–24, 2019.
96. Zhong, Y. and K. Hu, "Contraction integral equation for three-dimensional electromagnetic inverse scattering problem," *J. Imaging*, Vol. 25, 1–17, 2019.
97. Leijssen, R., P. Fuchs, W. Brink, A. Webb, and R. Remis, "Developments in electrical-property tomography based on the contrast-source inversion method," *J. Imaging*, Vol. 25, 1–19, 2019.
98. Estatico, C., A. Fedeli, M. Pastorino, A. Randazzo, and E. Tavanti, "Microwave imaging of 3D dielectric structures by means of a Newton-CG method in  $L_p$  spaces," *Int. J. Antennas Propag.*, Vol. 2019, 1–15, 2019.
99. Afsari, A., A. Abbosh, and Y. H. Samii, "A rapid medical microwave tomography based on partial differential equations," *IEEE Trans. Antennas and Propag.*, Vol. 6, 5521–5535, 2018.
100. Ambrosanio, M., P. Kosmas, and V. Pascazio, "Exploiting wavelet decomposition to enhance sparse recovery in microwave imaging," *Proc. EUCAP*, Paris, France, 2017.
101. Semnani, A., I. T. Rekanos, and M. Moghaddam, "Solving inverse scattering problems based on truncated cosine Fourier and cubic B-spline expansions," *IEEE Trans. Antennas and Propag.*, Vol. 60, 5914–5923, 2012.
102. Ahmadabadi, H. and K. Forooghi, "Application of Fourier-Jacobi expansion to inverse scattering problem," *IEEE Antennas Wireless Propag. Lett.*, Vol. 16, 956–959, 2017.
103. Athira, A. R., T. A. Anjit, and P. Mythili, "A multi-illumination multi-frequency approach for early detection of breast tumor by mode-matching method," *Proc. International Conference on Advances in Computing and Communications (ICACC)*, Cochin, India, 2015.
104. Islam, M. A., A. Kiourti, and J. L. Volakis, "A novel method to mitigate real-imaginary image imbalance in microwave tomography," *IEEE Trans. Biomed. Engineering (Early Access)*, 2019.
105. Bevacqua, M., et al., "A method for quantitative imaging of electrical properties of human tissues from only amplitude electromagnetic data," *Inverse Prob.*, Vol. 35, 1–18, 2018.
106. Zakaria, A. and J. LoVetri, "The finite-element method contrast source inversion algorithm for 2D transverse electric vectorial problems," *IEEE Trans. Antennas and Propag.*, Vol. 60, 1–21, Oct. 2012.
107. Ostadrahimi, M., A. Zakaria, J. LoVetri, and L. Shafai, "A near-field dual polarized (TE-TM) microwave imaging system," *IEEE Trans. on Microwave Theory and Tech.*, Vol. 61, 1376–1384, 2013.
108. Tzagkarakis, G., "Bayesian compressed sensing using Alpha-stable distributions," Ph.D. Thesis, Department of Computer Science, University of Crete, Nov. 2009.
109. Klemm, M., J. A. Leendertz, D. Gibbins, I. J. Craddock, A. Preece, and R. Benjamin, "Microwave radar-based differential breast cancer imaging: Imaging in homogeneous breast phantoms and low contrast scenarios," *IEEE Trans. Antennas and Propag.*, Vol. 58, 2337–2344, 2010.

110. Bourqui, J., J. Sill, and E. C. Fear, "A prototype system for measuring microwave frequency reflections from the breast," *Int. J. Biomed. Imaging*, Vol. 2012, 1–12, 2012.
111. Islam, M. T., M. Z. Mahmud, M. Tarikul Islam, S. Kibria, and M. Samsuzzaman, "A low cost and portable microwave imaging system for breast tumor detection using UWB directional antenna array," *Scientific Reports*, Vol. 9, 1–13, 2019.
112. Islam, M. T., M. Samsuzzaman, S. Kibria, N. Misran, and M. T. Islam, "Metasurface loaded high gain antenna based microwave imaging using iteratively corrected delay multiply and sum algorithm," *Scientific Reports*, Vol. 9, 1–14, 2019.
113. Alqadami, A. S. M., K. S. Bialkowski, A. T. Mobashsher, and A. Abbosh, "Wearable electromagnetic head imaging system using flexible wideband antenna array based on polymer technology for brain stroke diagnosis," *IEEE Trans. Biomed. Circuits Sys.*, Vol. 13, 124–134, 2019.
114. Manoufali, M., K. S. Bialkowski, N. Mohammed, P. C. Mills, and A. Abbosh, "Compact implantable antennas for the cerebrospinal fluid monitoring," *IEEE Trans. Antennas and Propag.*, Vol. 67, No. 8, 4955–4967, 2019.
115. Felicio, J. M., J. M. Biucas-Dias, J. R. Costa, and C. A. Fernandes, "Microwave breast imaging using dry setup," *IEEE Trans. Computational Imag.*, Vol. 6, 167–180, 2019.
116. Marimuthu, J., K. S. Bialkowski, and A. M. Abbosh, "Software-defined radar for medical imaging," *IEEE Trans. on Microwave Theory and Tech.*, Vol. 4, 643–652, 2016.
117. Stancombe, A. E., K. S. Bialkowski, and A. M. Abbosh, "Portable microwave head imaging system using software-defined radio and switching network," *IEEE Journal of Electromagnetics, RF and Microwaves in Medicine and Biology*, Vol. 3, No. 4, 284–291, 2019.
118. Casu, M. R., M. Vacca, J. A. Tobon, A. Pulimeno, I. Sarwar, R. Solimene, and F. Vipiana, "A COTS-based microwave imaging system for breast-cancer detection," *IEEE Trans. Biomed. Circuits Sys.*, Vol. 11, 804–814, 2017.
119. Porter, E., E. Kirshin, A. Santorelli, M. Coates, and M. Popovic, "Time-domain multistatic radar system for microwave breast screening," *IEEE Antennas Wireless Propag. Lett.*, Vol. 12, 229–232, 2013.
120. Wang, F. and T. Arslan, "Breast cancer detection with microwave imaging system using wearable conformal antenna arrays," *Proc. International Conf. Innovation Sustainability (IST)*, Gothenburg, Sweden, 2017.
121. Shao, W., A. Edalati, T. R. McColloug, and W. J. McCollough, "A phase confocal method for near-field microwave imaging," *IEEE Trans. on Microwave Theory and Tech.*, Vol. 65, 2508–2514, 2017.
122. Mukherjee, S., L. Udpa, S. Udpa, E. J. Rothwell, and Y. Deng, "A time reversal-based microwave imaging system for detection of breast tumors," *IEEE Trans. on Microwave Theory and Tech.*, Vol. 67, 2062–2075, 2019.
123. Oloumi, D., R. S. C. Winte, A. Kordzadeh, P. Boulanger, and K. Rambabu, "Microwave imaging of breast tumor using time-domain UWB circular-SAR technique," *IEEE Trans. Medical Imaging (Early Access)*, Vol. 39, No. 4, 934–943, 2019.
124. Kwon, S., H. Lee, and S. Lee, "Image enhancement with Gaussian filtering in time-domain microwave imaging system for breast cancer detection," *Electronics Lett.*, Vol. 52, 342–344, 2016.
125. Seo, Y., K. Sogo, and A. Toya, "CMOS equivalent time sampling of Gaussian monocycle pulse for confocal imaging," *2014 IEEE Biomedical Circuits and Systems Conference (BioCAS) Proceedings*, Lausanne, Switzerland, Oct. 22–24, 2014.
126. Li, X., E. J. Bond, B. D. Van Veen, and S. C. Hagness, "An overview of ultra-wideband microwave imaging via space-time beamforming for early-stage breast-cancer detection," *IEEE Antennas Propag. Mag.*, Vol. 47, 19–34, 2017.
127. Hossain, M. D., A. S. Mohan, and M. J. Abedin, "Beamspace time reversal microwave imaging for breast cancer detection," *IEEE Antennas Wireless Propag. Lett.*, Vol. 12, 241–244, 2013.

128. Li, Y., E. Porter, and M. Coates, "Imaging-based classification algorithms on clinical trial data with injected tumor responses," *Proc. EuCAP 2015*, 15, Lisbon, Portugal, May 2015.
129. Shahzad, A., M. O'Halloran, E. Jones, and M. Glavin, "A preprocessing filter for multistatic microwave breast imaging for enhanced tumor detection," *Progress In Electromagnetics Research B*, Vol. 57, 115–126, 2014.
130. Byrne, D. and I. J. Craddock, "Time-domain wideband adaptive beamforming for radar breast imaging," *IEEE Trans. Antennas and Propag.*, Vol. 63, 1725–1735, 2015.
131. O'Loughlin, D., B. L. Oliveira, M. Glavin, E. Jones, and M. O'Halloran, "Advantages and disadvantages of parameter search algorithms for permittivity estimation for microwave breast imaging," *Proc. Eucap 2019*, Krakow, Poland, 2019.
132. Li, Y., E. Porter, and M. Coates, "Imaging-based classification algorithms on clinical trial data with injected tumour responses," *Proc. EuCAP 2015*, 1–5, Lisbon, Portugal, 2015.
133. Elahi, M. A., B. R. Lavoie, E. Porter, M. Glavin, E. Jones, E. C. Fear, and M. O'Halloran, "Comparison of radar-based microwave imaging algorithms applied to experimental breast phantoms," *Proc. URSI GASS*, 1–4, Montreal, Canada, 2017.
134. Elahi, M. A., B. R. Lavoie, E. Porter, M. Glavin, E. Jones, E. C. Fear, and M. O'Halloran, "Evaluation of image reconstruction algorithms for confocal microwave imaging-application to patient data," *Sensors*, Vol. 18, 1–21, 2018.
135. O'Loughlin, D., B. L. Oliveira, M. Glavin, E. Jones, and M. O'Halloran, "Comparing radar-based breast imaging algorithm performance with realistic patient-specific permittivity estimation," *J. Imag.*, Vol. 5, 1–15, 2019.
136. Leith, E. N. and J. Upatnieks, "Reconstructed wavefronts and communication theory," *Journal of the Optical Society of America*, Vol. 52, 1123–1130, 1962.
137. Wang, L., R. Simpkin, and A. M. Al-Jumaily, "Holographic microwave imaging for medical applications," *J. Biomed. Science Engg.*, Vol. 6, 823–833, 2013.
138. Boriskin, A. and R. Sauleau, *Aperture Antennas for Millimeter and Sub-millimeter Wave Applications*, 490, Springer, 2017.
139. Amineh, R. K., M. Ravan, J. McCombe, and N. K. Nikolova, "Three-dimensional microwave holographic imaging employing forward-scattered waves only," *Intl. J. Antennas Propag.*, Vol. 2013, 1–16, 2013.
140. Amineh, R. K., J. McCombe, A. Khalatpour, and N. K. Nikolova, "Microwave holography using point-spread functions measured with calibration objects," *IEEE Trans. Instrum. Meas.*, Vol. 64, 403–417, 2015.
141. Amineh, R. K., M. Ravan, R. Sharma, and S. Baua, "Three-dimensional holographic imaging using single frequency microwave data," *Intl. J. Antennas Propag.*, Vol. 2018, 1–15, 2018.
142. Wang, L. and M. Fatemi, "Compressive sensing holographic microwave random array imaging of dielectric inclusion," *IEEE Access*, Vol. 6, 56477–56487, 2018.
143. Biabani, S. A. A., E. Shafie, and M. O. Khozium, "Indirect Holography Breast Cancer Detection System (IH-BCDS) using VORD," *European Scientific Journal*, Vol. 13, 10–21, 2017.
144. Elsdon, M., O. Yurduseven, and D. Smith, "Early stage breast cancer detection using indirect microwave holography," *Progress In Electromagnetics Research*, Vol. 143, 405–419, 2013.
145. Smith, D., O. Yurduseven, B. Livingstone, and V. Schejbal, "Microwave imaging using indirect holographic techniques," *IEEE Antennas Propag. Mag.*, Vol. 56, 104–117, 2014.
146. Tajik, D., "Advances in quantitative microwave holography," Ph.D. Thesis, Department of Electrical & Computer Engineering, McMaster University, Canada, 2017.
147. Fear, E. C., "Microwave imaging of the breast," *Technology in Cancer Research & Treatment*, Vol. 4, 69–89, 2005.
148. Kruger, R. A., K. K. Kopecky, A. M. Aisen, P. R. Reinecke, G. A. Kurger, and W. L. Kiser, "Thermoacoustic CT with radio waves: A medical imaging paradigm," *Radiology*, Vol. 211, 275–278, 1999.

149. Kruger, R. A., W. L. Kiser, P. R. Reinecke, and G. A. Kurger, "Thermoacoustic computed tomography using a conventional linear transducer array," *Intl. J. Med. Phy. Research & Practice*, Vol. 30, 856–860, 2003.
150. Zanger, G., O. Scherzer, and M. Haltmeier, "Circular integrating detectors in photo and thermoacoustic tomography," *Inverse Prob. Sci. Engg.*, Vol. 17, 133–142, 2009.
151. Xu, M., Y. Xu, and L. Wang, "Time-domain reconstruction algorithms and numerical simulations for thermoacoustic tomography in various geometries," *IEEE Trans. Biomed. Engineering*, Vol. 50, 1086–1099, 2003.
152. Ye, F., Z. Ji, W. Ding, C. Lou, S. Yang, and D. Xing, "Ultrashort microwave-pumped real-time thermoacoustic breast tumor imaging system," *IEEE Trans. Medical Imaging*, Vol. 35, 839–844, 2016.
153. Xu, X. and L. V. Wang, "Signal processing in scanning thermo-acoustic tomography in biological tissue," *Med. Phys.*, Vol. 28, 1519–1524, 2008.
154. Abbosh, Y. M., "Breast cancer diagnosis using microwave and hybrid imaging methods," *International Journal of Computer Science & Engineering Survey*, Vol. 5, 41–48, 2014.
155. Golnabi, A. H., P. M. Meaney, and K. D. Paulsen, "3D microwave tomography of the breast using prior anatomical information," *Med. Phys.*, Vol. 43, 1933–1944, 2016.
156. Golnabi, A. H., P. M. Meaney, S. D. Geimer, and K. D. Paulsen, "3-D microwave tomography using the soft prior regularization technique: Evaluation in anatomically-realistic MRI-derived numerical breast phantoms," *IEEE Trans. Biomed. Engineering*, Vol. 66, No. 9, 2566–2575, 2019.
157. Dagheyan, A. G., A. Molaei, R. Obermeier, A. K. Martinez, and J. M. Lorenzo, "Near-field radar microwave imaging as an add-on modality to mammography," *New Perspectives in Breast Imaging*, 15–43, Intech-Open Publishing, London, UK, 2017.
158. Jiang, H., et al., "Ultrasound-guided microwave imaging of breast cancer: Tissue phantom and pilot clinical experiments," *Med. Phys.*, Vol. 32, 2528–2535, 2005.
159. Massey, H., N. Ridley, and I. Lyburn, "Radiowave detection of breast cancer in the symptomatic clinic — A multi-centre study," *Proc. International Cambridge Conf. on Breast Imaging*, Cambridge, UK, Jul. 2017.
160. Ridley, N., M. Shere, and I. Lyburn, "Cancer detection in dense tissue using radiofrequency imaging—a clinical evaluation," *Proc. European Congress of Radiology Annual Meeting*, 1–9, Vienna, Austria, Mar. 2017.
161. Grzegorzczak, T. M., P. M. Meaney, and K. D. Paulsen, "Microwave tomographic imaging for breast cancer chemotherapy monitoring," *Proc. EuCAP 2014*, 702–703, Hague, Netherlands, 2014.
162. Meaney, P. M. and K. D. Paulsen, "Addressing multipath signal corruption in microwave tomography and the influence on system design and algorithm," *J. Biomed. Eng. Biosci.*, Vol. 1, 1–13, 2018.
163. Meaney, P. M., et al., "System and method using precious-metal nanoparticle contrast agent for microwave medical imaging," Patent No. US 9, 786, 048 B2, 2017.
164. Hosseinzadegan, S., A. Fhager, M. Persson, and P. M. Meaney, "A discrete dipole approximation solver based on the COCG-FFT algorithm and its application to microwave breast imaging," *International Journal of Antennas and Propagation*, Vol. 2019, 1–13, 2019.
165. Meaney, P. M., et al., "A 4-channel, vector network analyzer microwave imaging prototype based on software defined radio technology," *Rev. Sci. Instrum.*, Vol. 90, 1–14, 2019.
166. Fasoula, A., L. Duchesne, J. G. D. Cano, P. Lawrence, G. Robin, and J. G. Bernard, "On-site validation of a microwave breast imaging system, before first patient study," *Diagnostics*, Vol. 8, 1–38, 2018.
167. Fasoula, A., et al., "Microwave vision: From RF safety to medical imaging," *Proc. Eucap 2017*, 1–5, Paris, France, 2017.
168. Duchesne, L., A. Fasoula, E. Kaverine, G. Robin, and G. J. Bernard, "Wavelia microwave breast imaging: Identification and mitigation of possible sources of measurement uncertainty," *Eucap 2019*, 1–6, Krakow, Poland, 2019.

169. ICH GCP Clinical Trials Registry, "Pilot clinical evaluation of a microwave imaging system for early breast cancer detection pilot clinical study on a low-power electromagnetic wave breast imaging device for cancer screening purposes," <https://clinicaltrials.gov/ct2/show/NCT03475992>, accessed Jul. 2019.
170. Jeon, S., B. R. Kim, and S. H. Son, "Clinical trial of microwave tomography imaging," *Proc. URSI*, 1–2, Seoul, Korea, Aug. 2016.
171. Simonov, N., S. Jeon, B. R. Kim, K. J. Lee, and S. H. Son, "Advanced fast 3D electromagnetic solver for microwave tomography imaging," *IEEE Trans. Med. Imag.*, Vol. 36, 2160–2170, 2017.
172. Simonov, N., S. Jeon, B. R. Kim, and S. H. Son, "Analysis of the super-resolution effect on microwave tomography," *Special Issue — 2016 URSI Asia-Pacific Radio Science Conference*, 2019.
173. Porter, E., M. Coates, and M. Popovic, "An early clinical study of time-domain microwave radar for breast health monitoring," *IEEE Trans. Biomed. Engineering*, Vol. 63, 530–539, 2016.
174. Li, Y., E. Porter, A. Santorelli, M. Popovic, and M. Coates, "Microwave breast cancer detection via cost-sensitive ensemble classifiers: Phantom and patient investigation," *Biomedical Signal Processing and Control*, Vol. 31, 366–376, 2017.
175. Kranold, L., C. Quintyne, M. Coates, and M. Popovic, "Clinical study with a time-domain microwave breast monitor: Analysis of the system response and patient attributes," *Proc. Eucap 2013*, Krakow, Poland, 2019.
176. Yang, F., et al., "A large-scale clinical trial of radar-based microwave breast imaging for Asian women: Phase I," *IEEE International Symposium on Antennas and Propagation & USNC/URSI National Radio Science Meeting*, 781–783, San Diego, USA, 2017.
177. Bourqui, J. and E. C. Fear, "Systems for ultra-wideband microwave sensing and imaging of biological tissues," *Proc. EuCAP 2013*, 834–835, Gothenburg, Sweden, 2013.
178. Bourqui, J. and E. C. Fear, "Average breast permittivity measurements: Preliminary results from patient study," *Proc. EuCAP*, 1–4, Davos, Switzerland, 2016.
179. Ono, Y. and Kuwahara, "An analysis of microwave imaging using a combination of multi-static radar imaging and inverse scattering tomography methods," *IEEE Int. Symposium on Antennas & Prop. and USNC/URSI National Radio Science Meeting*, 2385–2386, San Diego, USA, 2017.
180. Song, H., et al., "Detectability of breast tumor by a hand-held impulse-radar detector: Performance evaluation and pilot clinical study," *Scientific Reports*, Vol. 7, 1–11, 2017.
181. Sasada, S., et al., "Portable impulse-radar detector for breast cancer: A pilot study," *Journal of Medical Imaging*, Vol. 5, 1–5, 2018.
182. Song, H., et al., "Microwave imaging using CMOS integrated circuits with rotating  $4 \times 4$  antenna array on a breast phantom," *International Journal of Antennas and Propagation*, Vol. 2017, 1–14, 2017.
183. Azhari, A., Y. Kuwano, X. Xiao, and T. Kikkawa, "Transmit/receive 320 GHz 1.2 mW packaged double-pole-16-throw switching matrix for radar-based target detection," *Japanese Journal of Applied Physics*, Vol. 57, 1–10, 2017.
184. Azhari, A. and T. Kikkawa, "A 2 to 12 GHz 65 nm transmit/receive CMOS DP8T switching matrix for ultra-wideband antenna arrays," *Int. J. Circ. Theor. Appl.*, Vol. 1–9, 2019.
185. Masui, Y., et al., "Gaussian monocycle pulse generator with calibration circuit for breast cancer detection," *Proc. BioCAS*, 1–4, Cleveland, OH, USA, 2018.
186. Sani, L., et al., "Novel microwave apparatus for breast lesions detection: Preliminary clinical results," *Science Direct Biomedical Signal Processing and Control*, Vol. 52, 257–263, 2019.
187. Vispa, A., et al., "UWB device for breast microwave imaging: Phantom and clinical validations," *Science Direct Measurement*, Vol. 146, 582–589, 2019.
188. Kobe University, "The science of looking beneath the surface," <https://kobeu.ac.jp/research-at-kobe/2019-06-17.html>, accessed Jan. 2020.
189. Kimura, et al., "Scattering tomography method and scattering tomography device," Patent Num. US 2016/0377557 A1, 2017.

190. Kimura, et al., "Scattering tomography method and scattering tomography device," Patent Num. EP 2 957 925 B1, 2016.
191. Hamsakutty, V., A. Lonappan, V. Thomas, G. Bindu, J. Jacob, J. Yohannan, and K. T. Mathew, "Coupling medium for microwave medical imaging applications," *Electronic Lett.*, Vol. 39, 1498–1499, 2003.
192. Amineh, R. K., M. Ravan, A. Trehan, and N. K. Nikolova, "Near-field microwave imaging based on aperture raster scanning with TEM horn antennas," *IEEE Trans. Antennas and Propag.*, Vol. 59, 928–940, 2011.
193. Mashal, A., et al., "Toward Carbon-nanotube-based theranostic agents for microwave detection and treatment of breast cancer: Enhanced dielectric and heating response of tissue-mimicking materials," *IEEE Trans. Biomed. Engineering*, Vol. 8, 1831–1834, 2010.
194. Mashal, A., B. Sitharaman, J. H. Booske, and S. C. Hagness, "Dielectric characterization of carbon nanotube contrast agents for microwave breast cancer detection," *Antennas and Propagation Society Int. Symp.*, 1–4, 2009.
195. Bevacqua, M. T. and R. Scapaticci, "A compressive sensing approach for 3D breast cancer microwave imaging with magnetic nanoparticles as contrast agent," *IEEE Trans. Med. Imag.*, Vol. 35, 665–673, 2016.
196. Samadishadlou, M., et al., "Magnetic carbon nanotubes: Preparation, physical properties, and applications in biomedicine," *Artificial Cells, Nanomedicine, and Biotechnology*, Vol. 7, 1314–1330, 2017.
197. Scapaticci, R., G. Bellizzi, I. Catapano, L. Crocco, and O. M. Bucci, "An effective procedure for MNP-enhanced breast cancer microwave imaging," *IEEE Trans. Biomed. Engineering*, Vol. 61, 1071–1079, 2014.
198. Bucci, O. M., G. Bellizzi, A. Borgia, S. Costanzo, L. Crocco, and D. G. Massa, "Characterization of a laboratory set-up for assessing the feasibility of magnetic nanoparticles enhanced microwave imaging," *Proc. EuCAP'16*, 1–4, Davos, Switzerland, 2016.
199. Akinci, M. N., M. Cayoren, and E. Gose, "Qualitative microwave imaging of breast cancer with contrast agents," *Phys. Med. Biol.*, Vol. 64, 1–12, 2019.
200. Mazri, T., F. Riouch, and N. A. Idrissi, "Design and simulation of a SP4T switch based on PIN diode suitable for UMTS use," *Int. J. Comp. Sci. Network Security*, Vol. 11, 77–81, 2011.
201. Wu, H. and R. K. Amineh, "A low-cost and compact three-dimensional microwave holographic imaging system," *Electronics*, Vol. 8, 1–20, 2019.
202. Nikolova, N. K., "Microwave imaging for breast cancer," *IEEE Microwave Mag.*, Vol. 12, 78–94, 2011.
203. Bucci, O. M. and G. Franceschetti, "On the degrees of freedom of scattered fields," *IEEE Trans. Antennas and Propag.*, Vol. 37, 918–926, 1989.
204. Kaye, C., I. Jeffrey, and J. LoVetri, "Improvement of multi-frequency microwave breast imaging through frequency cycling and tissue-dependent mapping," *IEEE Trans. Antennas and Propag.*, Vol. 67, 7087–7096, 2019.
205. Salucci, M., G. Oliveri, and A. Massa, "GPR prospecting through an inverse-scattering frequency-hopping multifocusing approach," *IEEE Trans. Geosci. Remote Sens.*, Vol. 53, 6573–6592, 2015.
206. Adler, J. and O. Oktem, "Solving ill-posed inverse problems using iterative deep neural networks," *Inverse Prob.*, Vol. 33, 1–24, 2017.
207. Sun, Y., Z. Xia, and U. S. Kamilov, "Efficient and accurate inversion of multiple scattering with deep learning," *Opt. Express*, Vol. 26, 14678–14688, 2018.
208. Data Science, "Why do convolutional neural networks work?" <https://datascience.stackexchange.com/questions/15903/why-do-the-convolutional-neural-networks-work>, accessed Nov. 2019.
209. Jin, K. H., M. T. McCann, and M. Unser, "Deep convolutional neural network for inverse problems in imaging," *IEEE Trans. Image Process.*, Vol. 26, 4509–4522, 2017.

210. Li, L., et al., "DeepNIS: Deep neural network for nonlinear electromagnetic inverse scattering," *IEEE Trans. Antennas and Propag.*, Vol. 67, 1819–1825, 2019.
211. Wei, Z. and X. Chen, "Deep-learning schemes for full-wave nonlinear inverse scattering problems," *IEEE Trans. Geosci. Remote Sens.*, Vol. 57, 1849–1860, 2019.
212. Sanghvi, Y., Y. Kalepu, and U. K. Khankhoje, "Embedding deep learning in inverse scattering problems," *IEEE Trans. Computational Imag.*, Vol. 6, 46–56, 2019.
213. Rana, S. P., et al., "Machine learning approaches for automated lesion detection in microwave breast imaging clinical data," *Scientific Reports*, Vol. 9, 1–12, 2019.
214. Ashtiani, F., A. Risi, and F. Aflatouni, "Single-chip nanophotonic near-field imager," *Optica*, Vol. 6, 1255–1260, 2019.